



## Calhoun: The NPS Institutional Archive

---

Theses and Dissertations

Thesis Collection

---

1986-12

# A numerical method for solving for normal modes with impedance bottom

Cantley, Douglas

---

<http://hdl.handle.net/10945/22006>



Calhoun is a project of the Dudley Knox Library at NPS, furthering the precepts and goals of open government and government transparency. All information contained herein has been approved for release by the NPS Public Affairs Officer.

**Dudley Knox Library / Naval Postgraduate School  
411 Dyer Road / 1 University Circle  
Monterey, California USA 93943**

<http://www.nps.edu/library>







DUDLEY KNOX LIBRARY  
NATIONAL POSTGRADUATE SCHOOL  
1001 Tenth Avenue, Suite 2000















# NAVAL POSTGRADUATE SCHOOL

Monterey, California



## THESIS

A NUMERICAL METHOD FOR SOLVING FOR  
NORMAL MODES WITH IMPEDANCE BOTTOM

by

Douglas Cantley

December 1986

Thesis Advisor:  
Co-advisor:

Alan B. Coppens  
Thomas B. Gabrielson

Approved for public release; distribution is unlimited

T230160



## REPORT DOCUMENTATION PAGE

REPORT SECURITY CLASSIFICATION Unclassified			1b. RESTRICTIVE MARKINGS			
SECURITY CLASSIFICATION AUTHORITY			3 DISTRIBUTION/AVAILABILITY OF REPORT Approved for public release; distribution is unlimited.			
DECLASSIFICATION/DOWNGRADING SCHEDULE						
PERFORMING ORGANIZATION REPORT NUMBER(S)			5 MONITORING ORGANIZATION REPORT NUMBER(S)			
NAME OF PERFORMING ORGANIZATION Naval Postgraduate School		6b OFFICE SYMBOL (If applicable) 61	7a NAME OF MONITORING ORGANIZATION Naval Postgraduate School			
ADDRESS (City, State, and ZIP Code) Monterey, California 93943-5000			7b. ADDRESS (City, State, and ZIP Code) Monterey, California 93943-5000			
NAME OF FUNDING/SPONSORING ORGANIZATION		8b. OFFICE SYMBOL (If applicable)	9 PROCUREMENT INSTRUMENT IDENTIFICATION NUMBER			
ADDRESS (City, State, and ZIP Code)			10 SOURCE OF FUNDING NUMBERS			
			PROGRAM ELEMENT NO	PROJECT NO	TASK NO	WORK UNIT ACCESSION NO
TITLE (Include Security Classification) A NUMERICAL METHOD FOR SOLVING FOR NORMAL MODES WITH IMPEDANCE BOTTOM						
PERSONAL AUTHOR(S) Cantley, Douglas						
1. TYPE OF REPORT Master's Thesis		13b TIME COVERED FROM _____ TO _____		14 DATE OF REPORT (Year, Month, Day) 1986 December		15 PAGE COUNT 99
SUPPLEMENTARY NOTATION						
COSATI CODES			18 SUBJECT TERMS (Continue on reverse if necessary and identify by block number) Normal Modes; Fast Field Program; Impedance Bottom; Propagation Loss			
FIELD	GROUP	SUB-GROUP				
ABSTRACT (Continue on reverse if necessary and identify by block number) This thesis describes the development of a computer program that calculates the propagation loss for low frequencies in a shallow ocean given the depth of source and receiver, the sound speed profile of the water, the frequency of the source, and the impedance and sound speed in the bottom. The program does this by computing the sum of normal modes for a specified set of boundary conditions. At the surface, perfect pressure release is assumed, and the boundary condition at the bottom is one of impedance mismatch. An effort was made to develop a Fast Field Program, which would use a FFT to predict propagation loss at a variety of ranges by solving for a discrete set of wave numbers, but development was not completed.						
DISTRIBUTION/AVAILABILITY OF ABSTRACT <input checked="" type="checkbox"/> UNCLASSIFIED/UNLIMITED <input type="checkbox"/> SAME AS RPT <input type="checkbox"/> DTIC USERS				21 ABSTRACT SECURITY CLASSIFICATION Unclassified		
NAME OF RESPONSIBLE INDIVIDUAL Alan B. Coppens				22b TELEPHONE (Include Area Code) 408-646-2941	22c. OFFICE SYMBOL 61cz	

Approved for public release; distribution is unlimited

A Numerical Method for Solving for  
Normal Modes with Impedance Bottom

by

Douglas Cantley  
Captain, Canadian Armed Forces  
B.A., University of Prince Edward Island, 1973

Submitted in partial fulfillment of the requirements for the degree of

MASTER OF SCIENCE IN ENGINEERING ACOUSTICS

from the

NAVAL POSTGRADUATE SCHOOL

December 1986



## ABSTRACT

This thesis describes the development of a computer program that calculates the propagation loss for low frequencies in a shallow ocean given the depth of source and receiver, the sound speed profile of the water, the frequency of the source, and the impedance and sound speed in the bottom. The program does this by computing the sum of normal modes for a specified set of boundary conditions. At the surface, perfect pressure release is assumed, and the boundary condition at the bottom is one of impedance mismatch. An effort was made to develop a Fast Field Program, which would use a FFT to predict propagation loss at a variety of ranges by solving for a discrete set of wave numbers, but development was not completed.

## TABLE OF CONTENTS

I.	INTRODUCTION .....	8
II.	THEORY .....	13
	A. DERIVATION OF THE FIELD INTEGRAL .....	14
	B. NORMAL MODE METHOD FOR PRESSURE DETERMINATION .....	19
	C. DIRECT EVALUATION OF THE FIELD INTEGRAL .....	24
	D. ABSORPTION AND BOUNDARY EFFECTS .....	27
III.	DESCRIPTION OF PROGRAMS .....	33
	A. NORMAL MODE PROGRAM .....	34
	B. FAST FIELD PROGRAM .....	37
IV.	TESTS RUN ON PROGRAMS .....	39
	A. RIGID BOTTOM WITH NO ABSORPTION .....	40
	B. RIGID BOTTOM WITH ABSORPTION .....	51
	C. IMPEDANCE BOTTOM .....	63
V.	CONCLUSIONS AND RECOMMENDATIONS .....	78
APPENDIX A	MATRIX METHOD FOR FINDING HORIZONTAL WAVE NUMBER .....	81
APPENDIX B	COMPUTER PROGRAM EXACT .....	83
APPENDIX C	COMPUTER PROGRAM FFP .....	91
	LIST OF REFERENCES .....	96
	INITIAL DISTRIBUTION LIST .....	97

## LIST OF TABLES

4.1	EVALUATION OF ACCURACY OF SUBROUTINE 'EIGENS' .....	41
4.2	RESULTS FROM 'EIGENS' WITH GRADIENT AND WITH DUCTS .....	43
4.3	PRESSURE COMPARISON - FFP VERSUS EXACT .....	59
4.4	EXACT - NUMBER OF INCREMENTS AND CORRECTION FACTOR .....	66
4.5	EXACT WITH IMPEDANCE BOTTOM .....	68
4.6	EXACT SOLUTIONS VARYING CRITICAL ANGLES .....	70

## LIST OF FIGURES

1.1	Methods of Solving for the Pressure Field .....	11
1.2	Solutions Derived from the Field Integral .....	12
3.1	Depth Function Divergence .....	36
4.1	Modal Pressure Variation with Depth .....	45
4.2	Relative Stimulation of Real Modes .....	46
4.3	Pressure Error Due to Wave Number Error .....	48
4.4	Modal Pressures with Small Range Change .....	49
4.5	Propagation Loss - No Absorption .....	50
4.6	Interference Patterns for Modes 1 and 3 .....	52
4.7	Propagation Loss with Variable Absorption .....	53
4.8	Propagation Loss for Sources at Varying Depths .....	54
4.9	FFP Wave Number Pressure Contributions - No Absorption .....	56
4.10	FFP Integral with Absorption .....	57
4.11	FFP Wave Number Contributions - Varying Number of Samples ...	60
4.12	FFP Integral with Varying Absorption .....	61
4.13	Modal Pressure Function with Impedance Bottom .....	64
4.14	Phase Shift/Bounce Versus Critical Angle .....	69
4.15	Loss/Bounce and Loss/Meter Versus Critical Angle .....	72
4.16	Mode 1 Pressure for Critical Angle 0.30 and 0.10 .....	73
4.17	Prop Loss - Critical Angle 0.1 Radian, 0.3 Radian .....	74
4.18	Prop Loss - Critical Angle 0.5 Radian, 0.9 Radian .....	75
4.19	Prop Loss for Iso-Speed and Positive Gradient .....	77

## ACKNOWLEDGEMENTS

I am deeply indebted to Dr. Tom Gabrielson whose teaching stimulated my interest in this topic and whose encouragement and direction made this thesis a meaningful experience. His leadership and example, together with a professional credo that knowledge involves much more than a familiarity with a library of complex formulae, inspire all who know him as a scientist or as a teacher. Dr. Alan Coppens proved a welcome source of knowledge and assistance. His patience and support were essential to the completion of this thesis.

I also wish to express my gratitude to the officers of the Canadian Armed Forces who made it possible for me to partake of this unique educational and professional experience.

Not least, I thank my wife, Birgit, for her unselfish support and understanding.



## I. INTRODUCTION

A wide variety of methods are available for determining the pressure field from a point source in a stratified ocean of constant depth. Figure 1.1 shows that, by using various transforms, it is possible to derive expressions describing the pressure field in terms of the linear wave equation, the Helmholtz equation and, finally, the field integral. Methods associated with these expressions vary, and each has relative advantages and disadvantages in terms of speed, accuracy, and ability to deal with complex situations. Unfortunately, no single method is superior in all respects and there must be trade-offs. In some situations, accuracy might be sacrificed for speed, or the ability to deal with unusual boundaries may override the importance of speed or accuracy.

Figure 1.2 shows the common methods of solving the field integral to determine the pressure. The Normal Mode Solution, the Method of Steepest Descent, The Multiple Scattering Method and Direct Numerical Integration are "exact" methods. The Fast Field Program (FFP), a method of numerical integration, must be considered an approximation, not only because it approximates a Hankel function by an exponential, but also because of its reliance on a finite number of samples. Since Stationary Phase normally requires approximations, then so does its derivative, the Method of Images. The Wentzel-Kramers-Brillouin (WKB) Integral normally involves approximations so both Ray Theory and the WKB Mode Equation will seldom be exact. It is possible to find exact solutions using the

Normal Mode Technique, but in this paper, as will be seen in Chapter II, practical assumptions relegate the solutions to the approximate category. This thesis is limited to consideration of the Normal Mode Solution, which is computed by the program EXACT, and a Fast Field Program, computer program FFP.

Chapter II derives the field integral, then develops the Normal Mode Solution, and describes the Fast Field Program, FFP. The basic difference between the methods involves the requirement of the Normal Mode Solution for an accurate estimation of the horizontal wave numbers for each of the modes. The FFP does not calculate the modal wave numbers but computes the pressure contributions for a large number of predefined horizontal wave numbers. An expression to describe losses and phase shift in terms of the impedance and sound speed ratios between the bottom and the water is also derived in Chapter II.

Chapter III describes the programs EXACT and FFP. EXACT solves the field integral by first finding good approximations of the mode wave numbers using a matrix eigenvalue technique and then refining them. FFP calculates the pressure field at a discrete number of horizontal wave numbers without regard to modal values. Both programs use the vector sum of the components of pressure from the constituent wave numbers to calculate the propagation loss between the source and the receiver, taking into account absorption in the water, losses to the bottom, and phase changes at the surface and bottom.

Chapter IV describes the testing procedures and the results. Within this chapter the testing criteria are defined and the adaptive nature of the development process is discussed. Test results provided some very

instructive lessons which gave an insight into how normal modes can describe pressure variations in both the vertical and horizontal.

Chapter V discusses the results and some of the weaknesses of the program.

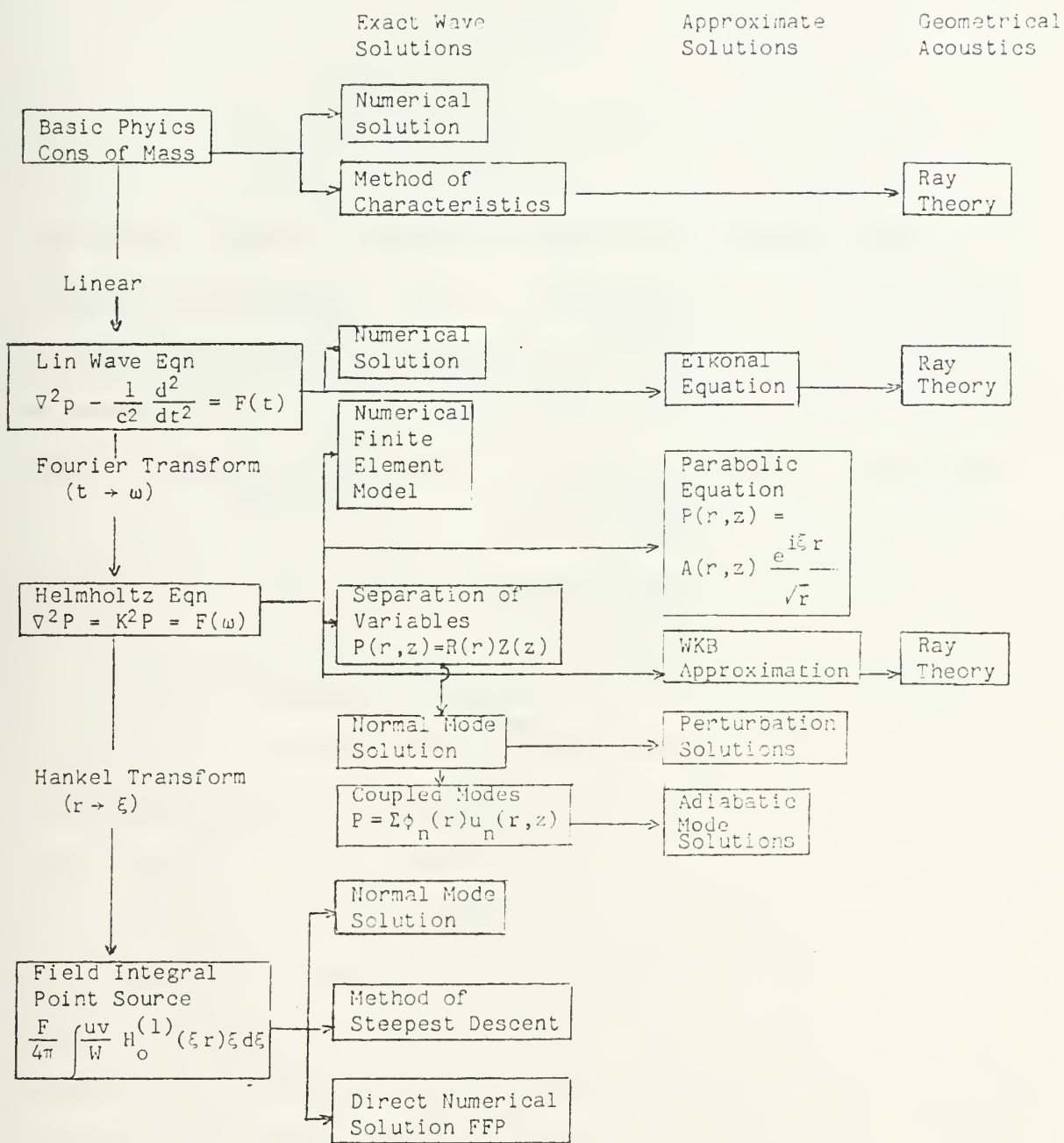


Figure 1.1. Methods of Solving for the Pressure Field.

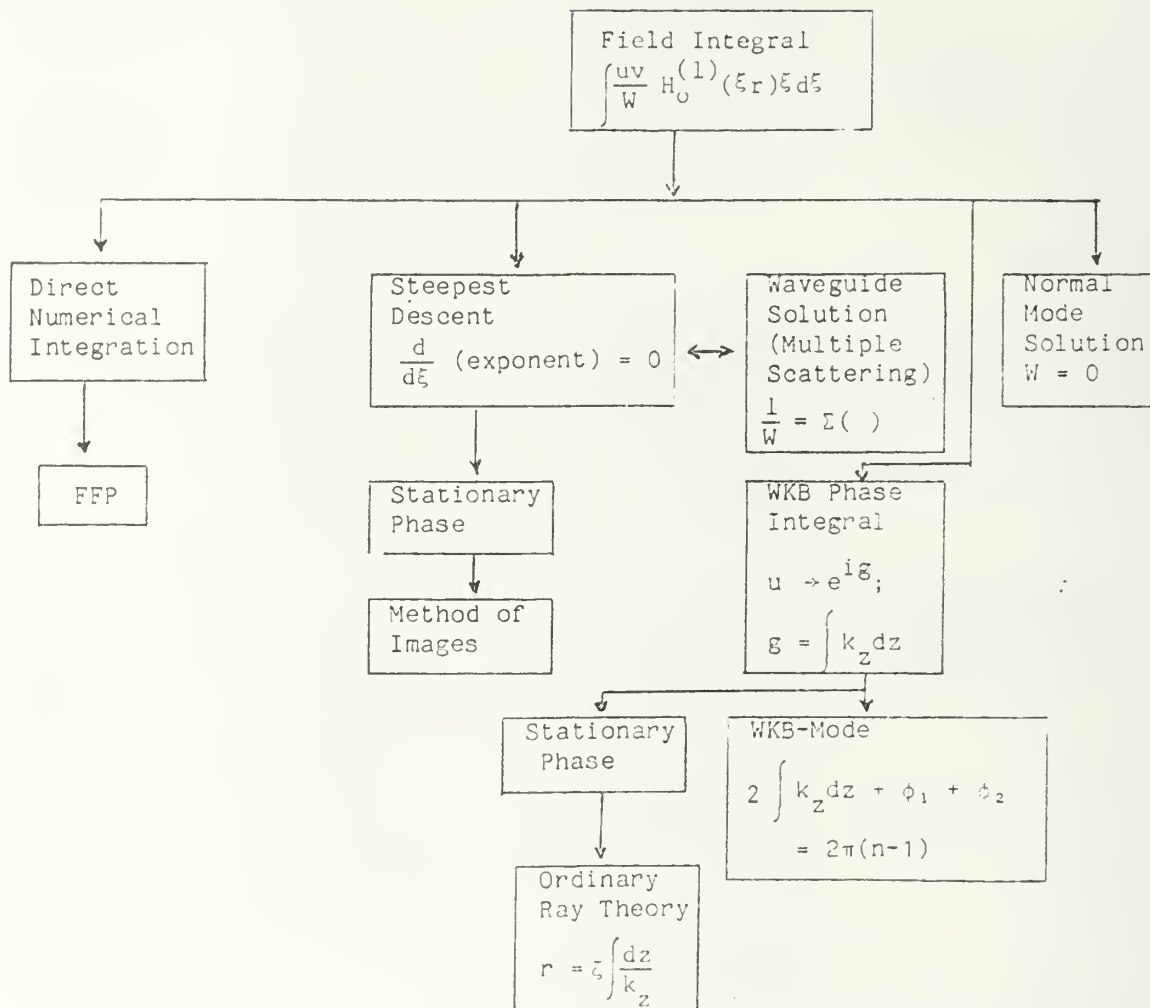


Figure 1.2. Solutions of the Wave Equation Derived from the Field Integral.



## II. THEORY

In this discussion of normal modes, frequency will be very low so the absorptive losses due to the water will be negligible, except at long ranges. However, absorption in the bottom will often be very high, especially for the higher modes. The theory was used to derive formulae for the lossless case; then absorption was introduced as an imaginary component of the horizontal wave number. Although absorption in the water is low for low frequencies, it proved expedient to input abnormally high absorption rates into the test programs. By doing this, it was possible to verify that the complex numbers were producing consistent values.

The theoretical approach involves a series of transforms, some of which require approximations for simplification. These transforms successively take the wave equation from the time domain to the frequency domain, from three dimensions to two, from range dependent to wave number dependent, and finally to a function that describes pressure as a function of the depths of the receiver and transmitter, the horizontal wave number and the horizontal range. Normal mode theory enables one to consider the total pressure as the sum of pressures from many components. Each mode is stimulated by the transmitter, or sensed by the receiver, to a degree that depends on the positions of the transmitter and receiver in relation to the modal depth function curve. This curve is described in Chapter IV.

In order to keep the program simple, several assumptions must be made; some limit the practicality of this particular program and could be overcome in a more comprehensive routine, while others are of little consequence.

The main assumptions, some of which will be discussed in detail later, are:

1. source is cw and monochromatic; it emits a continuous wave at a constant frequency;
2. source is a point radiating uniformly in all directions;
3. medium is homogeneous in all respects in the horizontal;
4. bottom and surface are flat and parallel;
5. surface is perfectly reflecting;
6. bottom can be completely described by its impedance;
7. all energy transmitted into the bottom is lost, and
8. branch line integrals can be ignored.

#### A. THE FIELD INTEGRAL

An omnidirectional point source operating at frequency  $f(t)$  is positioned at a depth  $z$  in a water mass that is uniformly homogeneous in sound speed in the horizontal plane and can be described in the vertical plane by the sound speed,  $c(z)$ , at any depth.

As long as the variations are linear, the pressure is given by the acoustic wave equation:

$$\nabla^2 p - \frac{1}{c^2(z)} \frac{d^2 p}{dt^2} = -f(t) \delta(\bar{s} - \bar{s}_0) \quad 2.1$$

where:

$p = p(\bar{s}, t)$  pressure as a function of position and time,

$f(t)$  = function describing the source amplitude,

$c(z)$  = depth dependent sound speed, and

$\bar{S}$  = position in Cartesian coordinates.

A Fourier transform from time to frequency,  $\omega$ , corresponds to considering the equation for distinct frequencies and yields:

$$\nabla^2 P + \frac{\omega^2}{c^2(z)} P = -F(\omega) \delta(\bar{S} - \bar{S}_0) \quad 2.2$$

where:

$P = P(\bar{S}, \omega)$  a function of position and frequency,

$\omega$  = frequency in radians/sec, and

$F(\omega)$  = transform of the driving function,  $f(t)$ .

Because the sound field is independent of the azimuthal angle, this transform can be formulated in the more manageable cylindrical co-ordinate system. In the new system the wave equation appears as:

$$\frac{\partial^2 P}{\partial r^2} + \frac{1}{r} \frac{\partial P}{\partial r} + \frac{\partial^2 P}{\partial z^2} + k^2 P = -F(\omega) \frac{\delta(z - z_0)}{2\pi r} \quad 2.3$$

where:

$k$  = wave number,  $\frac{\omega}{c(z)}$ ,

$z$  = depth, and

$P = P(r, z, \omega)$ , a function of horizontal range, depth and frequency.

The Hankel transform allows one to compute the changes of pressure with a change of depth, independent of the range. It requires consideration of the vertical component of the wave number,  $k_z$ :

$$\frac{\partial^2 \tilde{p}}{\partial z^2} + k_z^2 \tilde{p} = -\frac{F}{2\pi} \delta(z-z_0) . \quad 2.4$$

where:

$\tilde{p} = \tilde{p}(\xi, r, \omega)$  a function of horizontal wave number, horizontal range and frequency,

$$k_z^2 = k^2 - \xi^2$$

$\xi$  = horizontal wave number, and

$k$  = wave number,  $\frac{\omega}{c(z)}$ .

This equation is then solved by variation of parameters. Let

$$\tilde{p} = w_1(z)u(z) + w_2(z)v(z) \quad 2.5$$

where:

$$w_1(z) = -\frac{F}{2\pi} \int_0^z \frac{v(z)\delta(z-z_0)dz}{W_{uv}} , \quad 2.5a$$

$$w_2(z) = \frac{F}{2\pi} \int_z^h \frac{u(z)\delta(z-z_0)dz}{W_{uv}} , \quad 2.5b$$

$$W_{uv} = u \frac{dv}{dz} - v \frac{du}{dz} \text{ (the Wronskian),} \quad 2.5c$$

and both  $u$  and  $v$  are solutions of the homogeneous form of equation 2.4.

Now if  $v(z)$  satisfies the upper boundary condition and  $u(z)$  satisfies the lower boundary condition, then:

$$w_1 = \begin{cases} -F \frac{v(z_0)}{2\pi W_{uv}} & z > z_0 \\ 0 & z < z_0 \end{cases} \quad 2.6a$$

and

$$w_2 = \begin{cases} F \frac{u(z_0)}{2\pi W_{uv}} & z < z_0 \\ 0 & z > z_0 \end{cases} \quad 2.6b$$

This means that the transformed pressure can be written in terms of depth dependent  $u(z)$  and  $v(z)$  as:

$$\tilde{p} = \frac{F}{2\pi} \frac{u(z_0)v(z)}{W_{uv}} \quad \text{for } z < z_0 \quad 2.7a$$

$$\tilde{p} = \frac{F}{2\pi} \frac{u(z)v(z_0)}{W_{uv}} \quad \text{for } z > z_0 \quad 2.7b$$

A convenient way of representing this is

$$\tilde{p} = \frac{F}{2\pi} \frac{u(z_>)v(z_<)}{W_{uv}} \quad 2.8$$

where:

$z_>$  represents the larger of  $z$  and  $z_0$ , and

$z_<$  represents the smaller of  $z$  and  $z_0$ .

To obtain the actual pressure one must next take the inverse Hankel transform of zero order:



$$p = \int_0^{\infty} \bar{p} J_0(\xi r) \xi d\xi \quad 2.9$$

$$= \frac{F}{2\pi} \int_0^{\infty} \frac{u(z_>)v(z_<)}{W_{uv}} J_0(\xi r) \xi d\xi \quad 2.10$$

Use is made of the fact that [Ref. 1]

$$J_0(\xi r) = 1/2 \left[ H_0^{(1)}(\xi r) + H_0^{(2)}(\xi r) \right] \quad 2.11$$

and

$$H_0^{(2)}(\xi r) e^{-i\pi} = -H_0^{(1)}(\xi r) \quad 2.12$$

It is then possible to express the field integral (Equation 2.10) in terms of a Hankel function of the first kind [Ref. 2]:

$$P = \frac{iF}{4\pi} \int_{-\infty}^{\infty} \frac{u(z_>)v(z_<)}{W_{uv}} H_0^{(1)}(\xi r) \xi d\xi \quad 2.13$$

The Hankel function can be approximated by

$$H_0^{(1)}(\xi r) = \sqrt{\frac{2}{\pi \xi r}} e^{i(\xi r - \pi/4)} \left( 1 + \frac{1}{i8\xi r} + \dots \right) \quad 2.14$$

Restricting this expansion to the first term makes the integral much more manageable but restricts the minimum horizontal range so that  $\xi r \gg 1$ :

$$P = \frac{F}{4\pi} \sqrt{\frac{2}{\pi r}} e^{-i\pi/4} \int_{-\infty}^{\infty} \frac{u(z_{>})v(z_{<})}{W_{uv}} e^{i\xi r \sqrt{\xi}} d\xi \quad 2.15$$

This field integral represents the pressure, within the limits imposed by truncating the expansion of the Hankel function. This integral forms the basis for the derivation of formulae describing pressure using two different numerical approaches. At this point, the approach to the normal mode solution, which will be used in the program EXACT, takes a different tack from the approach which will be used in the FFP solution and program.

## B. NORMAL MODE METHOD FOR PRESSURE DETERMINATION

In this paper the normal mode method refers to the process whereby approximations for the eigenvalue of a mode are successively refined by numerically integrating the square of a depth function across the depth. A correction term is developed from this integral and is used to refine the approximation until the correction is negligible.

Let the guess at the normal mode horizontal wave number,  $\xi_n$ , be  $\xi$ .

For  $\xi$ ,  $v(z)$  satisfies

$$v'' + k_z^2 v = 0 \quad 2.16a$$

where:

$$k_z^2 = k^2 - \xi^2$$

For  $\xi_n$ ,  $v_n(z)$  satisfies

$$v_n'' + k_{zn}^2 v = 0 \quad 2.16b$$

where

$$k_{zn}^2 = k^2 - \xi_n^2.$$

Multiplying 2.16a by  $v_n$  and 2.16b by  $v$  and subtracting yields

$$v_n v'' - v v_n'' + v v_n (k_z^2 - k_{zn}^2) = 0 \quad 2.17$$

Then

$$\frac{d}{dz} (v_n v' - v v_n') + v v_n (k^2 - \xi^2 - k^2 + \xi_n^2) = 0, \text{ or}$$

$$\frac{d}{dz} (v_n v' - v v_n') = (\xi^2 - \xi_n^2) v v_n. \quad 2.18$$

Integrating from depth 0 to depth h:

$$(v_n v' - v v_n') \Big|_0^h = (\xi^2 - \xi_n^2) \int_0^h v v_n dz \quad 2.19$$

or

$$v_n(h)v'(h) - v_n'(h)v(h) - v_n(0)v'(0) + v_n(0)v(0) = (\xi^2 - \xi_n^2) \int_0^h v v_n dz. \quad 2.20$$

The following argument holds for any set of permissible boundary conditions but, in order to clarify the discussion, the specific case of pressure release at  $z = 0$  and rigid at  $z = h$  will be selected. The function  $v(z)$  is not a mode, but it can be forced to satisfy one of the boundary conditions without losing generality. If  $v(z)$  is defined to satisfy the boundary condition at  $z = 0$ , then, for any permissible boundary condition, the last pair of terms on the left hand side of equation 2.20 is identically zero. Therefore,

$$v_n(h)v'(h) - v_n'(h)v(h) = (\xi^2 - \xi_n^2) \int_0^h v v_n dz. \quad 2.21$$

For the simplest case considered in this paper, the bottom boundary condition is rigid so that  $v_n'(h) = 0$ . Therefore

$$v_n(h)v'(h) = (\xi^2 - \xi_n^2) \int_0^h v v_n dz \quad 2.22$$

and, since  $v \approx v_n$  for  $\xi$  close to  $\xi_n$ ,

$$\Delta \xi^2 = \xi^2 - \xi_n^2 = \frac{v(h)v'(h)}{\int v^2 dz}$$

$$\xi_n^2 = \xi^2 - \frac{v(h)v'(h)}{\int v^2 dz} \quad 2.23$$

Besides proving useful in determining successively better approximations of  $\xi_n$ , this same integral forms part of the expression for the contribution of a mode, since it is proportional to the derivative of the Wronskian with respect to wave number.

The Cauchy integral enables one to write equation 2.13 as the sum of the residues of all the poles of the integrand. Each pole corresponds to a normal mode.

$$P = \frac{iF}{2\pi} \sum_n \frac{u_n v_n H_0^{(1)}(\xi_n r) \xi_n}{\left. \frac{dW}{d\xi} \right|_{\xi_n}} \quad 2.24$$

where:

$$W(\xi_n) = 0$$

To derive an expression for  $(dW/d\xi)$  multiply both sides by

$$\beta = \frac{u_n(h)}{v_n(h)} \quad (\beta \text{ also equals } \frac{u_n'}{v_n'})$$

$$u_n(h)v'(h) - u_n'(h)v(h) = (\xi - \xi_n)(\xi + \xi_n)\beta \int_0^h v^2 dz \quad 2.25$$

The left-hand side of this equation gives the Wronskian for  $u$  and  $v$ , and, as  $\xi \rightarrow \xi_n$ ,  $W(\xi_n) \rightarrow 0$ , as it should:

$$\left. \frac{dW}{d\xi} \right|_{\xi_n} = \lim_{\Delta\xi \rightarrow 0} \frac{\Delta W}{\Delta\xi} \quad 2.26$$

$$= \frac{W(\xi) - W(\xi_n)}{\xi - \xi_n} = \beta(\xi + \xi_n) \int_0^h v^2 dz \quad 2.27$$

Since  $\xi \sim \xi_n$ , and by properly constructing the program, the constant  $\beta$  can be forced to be equal to 1,

$$\left. \frac{dW}{d\xi} \right|_{\xi_n} = 2\xi_n \int_0^h v^2 dz \quad 2.28$$

and equation 2.24 can now be written:

$$P = \frac{iF}{2\pi} \sum_n \frac{u_n v_n}{2\xi_n \int v^2 dz} H_0^{(1)}(\xi_n r) \xi_n. \quad 2.29$$

Using the exponential for the Hankel function, as in eqn. 2.13:

$$P = \frac{iF}{4\pi} \sum_n \sqrt{\frac{2}{\pi\xi_n r}} \frac{u_n v_n}{\int v^2 dz} e^{i\xi_n r} e^{-i\pi/4} \quad 2.30$$

$$= \frac{F}{4\pi} \sum_n \sqrt{\frac{2}{\pi\xi_n r}} \frac{u_n v_n e^{i\xi_n r}}{\int v^2 dz} e^{i\pi/4} \quad 2.31$$



In reality, this only represents the pressure in a system for which there are no boundary losses: i.e., for self-adjoint boundary conditions.

If real losses, including scattering, were to be taken into account,

the term  $\int_0^h v^2 dz$  must be replaced by [Ref. 3]:

$$\int_0^h v^2 dz + \left[ v^2(0) \left( \frac{d\lambda}{d\xi} \right) - v^2(h) \left( \frac{d\mu}{d\xi} \right) \right] \quad 2.32$$

where:

$$\lambda = \frac{dv/dz}{v} \quad \mu = \frac{du/dz}{u}$$

Ignoring boundary losses, equation 2.31 represents the total pressure at a point which is at depth  $z$  and horizontal distance  $r$  from a point cw source at depth  $z_0$ . This equation is the basis of the computer program EXACT, which is discussed in detail in Chapter III.

#### C. DIRECT EVALUATION OF THE FIELD INTEGRAL

The second method of determining pressure at a point requires calculating the field integral itself and then numerically integrating. Equation 2.15 represents the pressure field in terms of the Wronskian and the source and receiver depth functions  $u(z)$  and  $v(z)$ . The integral is solved by replacing it with a summation across an interval of wave numbers. Pressure at a point is found to be the sum of the pressure contributions from each horizontal wave number:

$$P = \frac{F}{4\pi} \sqrt{\frac{2}{\pi r}} e^{-i\pi/4} \sum_{-\xi_n}^{\xi_n} \frac{u(z_>)v(z_<)}{W_{uv}} e^{im\Delta\xi r} \sqrt{m\Delta\xi} \Delta\xi \quad 2.33$$

$u(z_>)$ ,  $v(z_<)$ , and  $W_{uv}$  are calculated from the known boundary conditions at the surface and at the bottom.  $\Delta\xi$  must be small enough to ensure accuracy.

It is impractical to pursue this theme without introducing absorption. Evaluation of equation 2.34 when  $m\Delta\xi = \xi_n$  produces  $W_{uv} = 0$  in the denominator, leading to an infinite solution. The magnitude of  $P_n$  then depends on how near  $m\Delta\xi$  comes to  $\xi_n$ . Introduction of absorption as an imaginary component of horizontal wave number displaces the poles from the real axis and ensures that the Wronskian does not go to zero along the path of integration. This has the effect of dispersing the energy out of the theoretically limitless pressure function that results when the Wronskian goes to zero at the exact wave number corresponding to the normal modes.

The terms within the summation sign of equation 2.33 have the same form as the discrete Fourier transform, normally considered for time,  $t$ , and frequency,  $\omega$ :

$$\sum_{n=0}^{N-1} G(n\Delta\omega) e^{i2\pi nm/N} = g(m\Delta t). \quad 2.34$$

By simply renaming the variables, the transform becomes:

$$\sum_{n=0}^{N-1} G(n\Delta\xi) e^{i2\pi nm/N} = g(m\Delta r). \quad 2.35$$

This is the basis for the technique known as the Fast Field Program [Ref.4]. By comparing equation 2.34 to equation 2.35, the following can be seen to be true:

$$G(n\Delta\xi) = \frac{uv}{W} \xi \Big|_{\xi=n\Delta\xi} \quad 2.36$$

The pressure at range R can then be written as

$$P_R = P_{m\Delta r} = \frac{F}{4\pi} \sqrt{\frac{2}{\pi m\Delta r}} e^{-i\pi/4} \Delta\xi [\text{FFT}[G]]. \quad 2.37$$

The capability of this Fast Field Program will be limited by the number of range (and wave number) increments. The wave number sampling increment,  $\Delta\xi$ , the range resolution,  $\Delta r$ , and the number of points in the FFT can be seen to be related by:

$$\frac{2\pi nm}{N} = \xi r = (n\Delta\xi)(m\Delta r) \quad 2.38$$

or

$$\frac{2\pi}{N} = \Delta\xi \Delta r, \quad 2.39$$

which results from comparing equations 2.34 and 2.35. The number of sampling points, N, places practical limits on either the maximum range or the range resolution.

#### D. ABSORPTION AND BOUNDARY EFFECTS

Sound energy is "lost" by absorption in the water and transmission into the bottom. In both cases a primary variable is frequency but the angle of travel of the mode and the type of bottom must be taken into account. This paper limits discussion to a non-scattering surface, water volume and bottom. It also neglects energy that is transmitted into the bottom and then returned to the water after refraction within the bottom.

Sound absorption in the water at low frequencies (under 1 KHz) is due primarily to relaxation of the boric ion. Standard texts [Refs. 5,6] define absorption in this frequency range as:

$$a = \frac{0.1F^2}{1+F^2} \quad 2.40$$

where:

a = absorptive loss in dB/m, and

F = frequency in kilohertz.

This loss can be converted to the fractional loss,  $\alpha$ , for a given distance in nepers/meter:

$$\text{Loss} = 20 \log_{10} e^{a r} \text{ dB}$$

$$a r = 20 \log_{10} e^{a r}$$

$$= 20 a r \log_{10} e$$

$$= 8.7 \alpha r$$

$$a = 8.7\alpha \text{ dB/meter, or } \alpha = \frac{a}{8.7} \text{ nepers/meter} \quad 2.42$$

This loss rate can be introduced into the equations derived earlier by adding absorption as an imaginary component of the wave number:

$$k_c = k + i\alpha \quad 2.42$$

The exponential form provides the absorptive loss factor:

$$\begin{aligned} e^{ik_c R} &= e^{i(k+i\alpha)R} \\ &= e^{ikR} e^{-\alpha R} \end{aligned} \quad 2.43$$

However, all of the expressions for pressure are given in terms of the horizontal range,  $r$ , not actual "path" length,  $R$ . Since  $\frac{\xi}{k} = \frac{r}{R}$ , the loss factor can be written as:

$$\text{loss} = e^{-\alpha \frac{k}{\xi} r} \quad 2.44$$

Bottom interactions cause losses and phase changes which must be taken into account. In their discussion of propagation loss using normal modes and an impedance boundary condition, Koch and Lindberg [Ref. 7] begin their discussion by defining the relationship between pressure and its derivative with respect to depth:

$$\frac{dP}{dz} = ik_z \frac{1-R}{1+R} P, \quad 2.45$$

where

$P$  = fluid pressure in the water at the boundary,

$\frac{dP}{dz}$  = derivative of pressure with respect to depth,

$k_z$  = vertical wave number, and

$R$  = complex reflection (Rayleigh) coefficient.

The Rayleigh reflection coefficient for the boundary between two homogeneous fluids is given [Ref. 5, Equation 6.30] by:

$$R = \frac{\frac{\rho_b c_b}{\rho_w c_w} - \frac{\sin \theta_b}{\sin \theta_w}}{\frac{\rho_b c_b}{\rho_w c_w} + \frac{\sin \theta_b}{\sin \theta_w}} \quad 2.46$$

where

$c_b$  = sound speed in the bottom at the interface,

$c_w$  = sound speed in the water at the interface,

$\rho_w$  = density of water,

$\rho_b$  = density of the bottom,

$\theta_w$  = angle, measured from the horizontal at which the wave strikes the

bottom, and

$\theta_b$  = angle, measured from the horizontal, at which the wave is transmitted into the bottom.

Substituting this value of  $R$  into Equation 2.45 and simplifying:

$$\frac{dP}{dz} = ik_z \frac{\rho_w c_w}{\rho_b c_b} \frac{\sin \theta_b}{\sin \theta_w} P. \quad 2.47$$

But

$$\sin \theta_b = \sqrt{1 - \cos^2 \theta_b} \quad 2.48$$

Snell's Law relates the incident and transmitted angles by:

$$\cos \theta_b = \frac{c_b}{c_w} \cos \theta_w \quad 2.49$$

So,

$$\sin \theta_b = \sqrt{1 - \frac{c_b^2}{c_w^2} \cos^2 \theta_w}. \quad 2.50$$

The critical angle,  $\theta_c$ , is defined as that grazing angle for which the transmitted angle is zero. This means that:

$$\frac{\cos \theta_w}{c_w} = \frac{\cos(0)}{c_b} \quad \text{and} \quad \frac{c_b}{c_w} = \frac{1}{\cos \theta_c}, \quad 2.51$$

where  $\theta_c$  is the critical grazing angle, measured from the horizontal.

Therefore, from Equation 2.50,

$$\sin \theta_b = \sqrt{1 - \frac{\cos^2 \theta_w}{\cos^2 \theta_c}}. \quad 2.52$$



By definition,

$$\cos \theta_w = \frac{\xi}{k} \quad 2.53$$

and

$$\sin \theta_w = \frac{k_z}{k} . \quad 2.54$$

Substituting Equations 2.52 and 2.54 into Equation 2.47:

$$\frac{dP}{dz} = ik \frac{\rho_w c_w}{\rho_b c_b} \sqrt{1 - \frac{\cos^2 \theta_w}{\cos^2 \theta_c}} P. \quad 2.55$$

In terms of wave numbers, Equation 2.53 can be used to give:

$$\frac{dP}{dz} = ik \frac{\rho_w c_w}{\rho_b c_b} \sqrt{1 - \frac{\xi^2}{k^2 \cos^2 \theta_c}} P \quad 2.56$$

or

$$\frac{dP}{dz} = i \frac{\rho_w c_w}{\rho_b c_b} \sqrt{k^2 - \frac{\xi^2}{\cos^2 \theta_c}} P. \quad 2.57$$

Equation 2.56 shows that, for any grazing angle less than critical, the pressure derivative will be real whereas, for grazing angles greater than critical, the derivative will be purely imaginary. If the pressure were complex, the derivative would be complex and complicated, too

complicated to solve in all cases with the basic program design. Therefore, only the real component of pressure was used in the determination of the boundary conditions.

A practical discussion of the physical significance of the reflection coefficient and the relationship amongst it, the grazing angle and critical angle is included in Chapter IV.

### III. PROGRAMS

Implementation of theory into the computer programs required two distinctly different methods. The program EXACT made accurate estimates of the normal mode horizontal wave numbers in order to compute the pressure as the sum of the pressure components from each of the modes. Absolute values of pressure are of no concern in either EXACT or FFP because the purpose is to compute propagation loss. It was assumed that forcing function,  $F$ , had a value of unity. The calculated pressure can then be compared to the pressure at one meter, and from that ratio, the propagation loss is calculable using decibel ratios. The program FFP did not compute horizontal wave numbers of modes; it assumed a large number of wave numbers equally spaced, calculated the pressure for each, and summed the individual contributions to give a final pressure.

Both programs were written using complex numbers and double precision (64 bit words), except for subroutine 'eigens' which was restricted to single precision because it relied upon IMSL routine EQRTIS which was available only in single precision.

Subroutines 'modes1' and 'modes2' provide many common functions for both programs EXACT and FFP. They calculate the transmitter and receiver modal pressure functions by stepping upward or downward from one of the boundaries, computing the pressure and its derivative with respect to depth by means of a fourth order Runge-Kutta technique [Ref.7].

## A. NORMAL MODE PROGRAM

This program is attached as Annex B. EXACT computes the approximate modal horizontal wave numbers by means of the subroutine 'eigens'. It then refines the horizontal wave number estimate to the desired accuracy using subroutine 'modes1' or 'modes2' and computes the pressure factors for each mode. Its aim is to compute the total pressure and, hence, the propagation loss at each range of interest.

Subroutine 'eigens' uses a matrix method [Ref.8] to approximate all the real modal horizontal wave numbers as well as the first evanescent mode. At the ranges of concern, it is unlikely that more than the first evanescent mode would be significant. The matrix of wave number estimates is found in a relatively short time and, although not guaranteed to be accurate, it is complete; no modes are skipped.

The next step involves finding the exact values of the horizontal wave number for each mode. The procedure utilizes the fact that, for each mode, both boundary conditions for a depth function ( $u$  or  $v$  from Chapter II) will be met. By setting the depth function or its derivative with respect to depth to a known boundary condition at the top or the bottom, it is possible to find a vertical wave number that will result in the boundary conditions being met at the the other boundary. The boundary with higher sound velocity will experience an exponential decay in the depth function. By starting at this boundary, it is a relatively simple matter to solve for vertical wave numbers that result in

sinusoidal variations that lead to solvable boundary conditions as the other boundary is approached. This avoids the possible problem that would exist if an attempt had been made to start at the boundary which had the lower sound velocity. In that case it is possible that instead of solving for an exponentially decaying function, the function may be exponentially growing, and no solution is possible. Figure 3.1 illustrates how a poor choice of starting boundary could lead to an unsolvable situation. For each of the modes in the 'main' routine calls either 'modes1' (when sound speed is greater at the top than at the bottom), or 'modes2' otherwise. It calls with starting estimates of the modal horizontal wave number; the value from 'eigens' the first time and an improved value each subsequent time.

'Modes1', using the best estimate for  $\xi_n$ , computes the modal depth function at each increment of depth, starting at the surface where the depth function is zero and its derivative with respect to depth is set to 1.0. The integral (Equation 2.31) is calculated at each interval and its final value at the bottom is used in the correction term.

At the bottom, the depth function and derivative are compared to the boundary conditions expected for a mode. For a rigid bottom, a derivative of zero is expected. For an impedance bottom, the expected derivative will be defined by Equation 2.56. The error in the derivative, together with the depth function and the integral is used to calculate a correction for the modal horizontal wave number.

If the surface sound speed is greater at the bottom than at the top, subroutine 'modes2' is called. It performs the same function as 'modes1' but starts at the bottom, where the depth function and derivative are

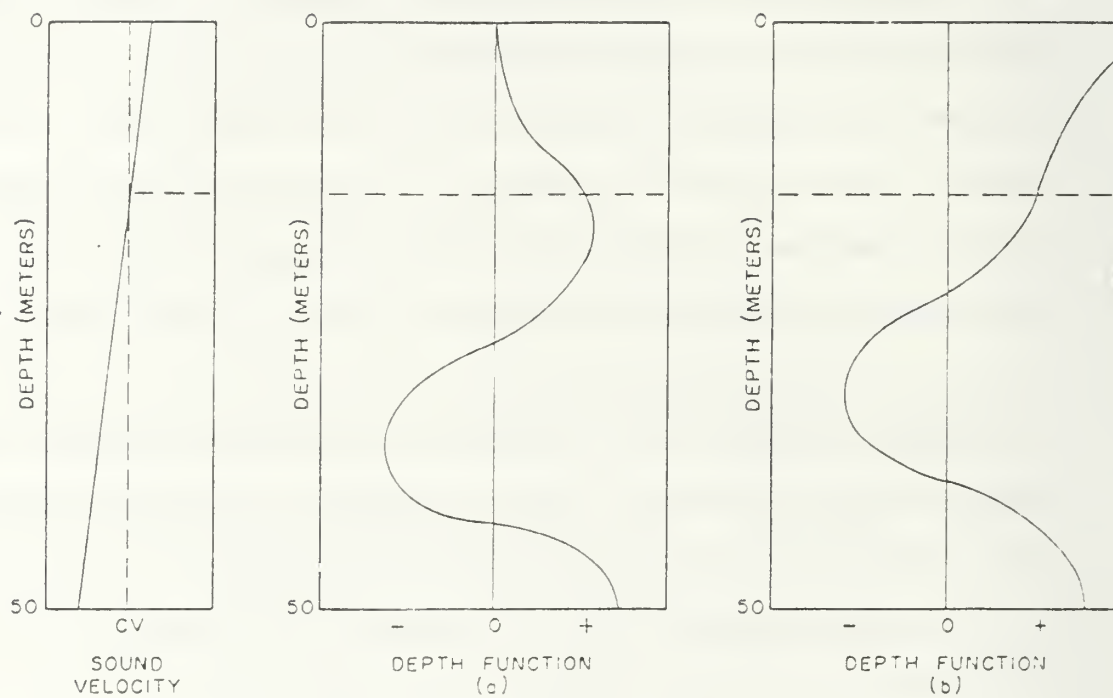


Figure 3.1. Possible Solutions to Depth Function Starting at:  
a: Boundary with Exponential (Convergent) and  
b: Boundary with Sinusoidal Changes (Possibly Divergent).

set to meet the boundary conditions for an impedance bottom (Equation 2.56). A correction is made after the subroutine has stepped to the surface and comparison has been made with modal boundary condition expectations; in this case depth pressure function equal to zero.

'Modes1' or 'modes2' will be repeatedly called until  $\xi_n$  has been satisfactorily estimated. The 'main' routine then computes the 'incomplete' modal pressure from the modal depth functions, the integral, and the horizontal wave number,  $\xi_n$ , (Equation 2.31) for each mode, storing them for later use. It is termed 'incomplete' because there is no range dependency at this point.

After the last mode has been processed by 'modes1' or 'modes2', range is introduced and partial pressures for each mode are calculated, keeping an updated sum (complex) of all the modal pressure factors. These pressure factors are then converted to propagation loss. It is a simple matter, once all the eigenvalues have been found, to compute the propagation loss for a series of ranges, as can be seen in Appendix B, Program EXACT.

## B. FAST FIELD PROGRAM

This program was written with the intent of completing a Fast Fourier Program, FFP, which would utilize a Fast Fourier Transform, FFT, subroutine. However, the program was only completed to the point where pressure factors were computed for individual ranges (as in EXACT), rather for a large number of ranges (as is the intent of an FFP). The computer program FFP, although incomplete, is included as Appendix C.



It was mentioned previously that EXACT and FFP are provided many common functions by 'modes1' and 'modes2'. There are also some basic differences in the way the subroutines are used by the two programs. In FFT, since no exact wave numbers are to be calculated, there is no requirement for subroutine 'eigens'. For the same reason, there is no requirement to find corrections to the wave numbers, so 'modes1' and 'modes2' are used differently. In fact, both subroutines are required by FFP.

Using the incremental wave number,  $n\Delta\xi$ , subroutine 'modes1' starts at the surface with the same boundary conditions as in EXACT and steps down, computing the pressure function and the derivative, through the depth of the upper of the transmitter or the receiver, and stops at the lower of the two. Values are required at the lower level for later use with the values from 'modes2' to calculate the Wronskian. Then 'modes2' starts at the bottom with the same boundary conditions as EXACT and steps upward until the pressure function and derivative have been calculated for the lower level.

The 'main' routine then uses the pressure functions and derivatives to calculate a partial pressure (Equation 2.33) for that wave number increment. Each partial pressure is summed (integrated) so that, when the last wave number has been processed, the result is the total pressure.

As in EXACT, FFP computes the propagation loss for each range. Implementation of the FFT would make it unnecessary to step through ranges as must be done with EXACT; propagation loss would be calculated for as many ranges as there are FFT points.

#### IV. TESTS RUN ON THE PROGRAM

Because it was difficult to gauge the correctness of the program or, more to the point, the veracity of this author's ideas, it was considered prudent to check the results at each stage of development. Although the process was awkward and time-consuming it proved necessary and resulted in some unexpected benefits; the results of some of the tests provided graphical insight into the phenomenon of sound propagation. By starting with isospeed conditions, verifications were simplified. Solutions for horizontal wave numbers which resulted from the computer programs were checked against 'correct' solutions from simple formulae for the non-absorption, rigid bottom system, as well as for the system that included absorption in the water. Once the impedance bottom was introduced, an analytic approach was required to decide if corrections were applied properly. A simple expedient to check on the program at any point involved plotting propagation loss against horizontal range for pairs of modes and observing the interference distance between nulls. This distance, when compared to the theoretical distance would highlight an error if there were an anomaly. Another check involved the observation that, for a shallow channel such as that used in the model, losses are generally spherical at short ranges and cylindrical for far ranges. The smoothed propagation loss curves could be expected to lie roughly along curves predicted on this basis.

The first tests involved studying the basic building blocks of the program. As the data were read from input files, they were printed into

a new file to ensure that correct information was being utilized. Another simple check involved printing a matrix of the wave numbers as they were computed. To illustrate the importance of such a basic check, it is worth remarking that the half-increment method required that the wave number be calculated for each half-increment of depth, including a depth of zero. Since the variation of Fortran used does not support a matrix with a zeroth element, a printout proved very useful in visualizing the situation and pin-pointing a subtle error. In many cases it was only by printing out all of the variables after each step that errors could be identified and remedied.

#### A. RIGID BOTTOM WITH NO ABSORPTION

Subroutine 'eigens' was first checked for correctness by comparing its constant speed solution, for each mode, to a solution which was known to be accurate. This accurate solution was based on the concept that, for a constant sound speed, with rigid bottom and no absorption, the pressure function would be sinusoidal, satisfying both boundary conditions. This means that the horizontal wave number for each mode (n always odd) can be defined in terms of the wave number, k, and the water depth, H:

$$\xi_n^2 = k^2 - \left(\frac{n\pi}{2H}\right)^2. \quad 4.1$$

Because the subroutine could only be run in single precision, high resolution was not expected. Table 4.1 shows that resolution increased linearly with the number of depth increments. For example, for mode 2, the

TABLE 4.1. SUBROUTINE 'EIGENS' - COMPUTED SQUARES OF WAVE NUMBERS AND ERRORS RESULTING FROM VARIATION OF NUMBER OF DEPTH INCREMENTS.

NUM OF INCRMT	MODE NUMBER			
	1	2	3	4
	VALUE ERROR	VALUE ERROR	VALUE ERROR	VALUE ERROR
25	0.2144624294 -0.0000906215	0.1959892982 -0.0009006298	0.1525131932 -0.0032877883	0.0237859429 -0.0614532906
50	0.2144174816 -0.0000456736	0.1955415049 -0.0004528365	0.1508744489 -0.0016490440	-0.0209414381 -0.0167259096
100	0.2143947361 -0.0000229281	0.1953157087 -0.0002270403	0.1500510807 -0.0008256757	-0.0305268121 -0.0071405356
200	0.2143832949 -0.0000114870	0.1952023429 -0.0001136746	0.1496385139 -0.0004131089	-0.0342955159 -0.0033718318
400	0.2143775572 -0.0000057492	0.1951455441 -0.0000568758	0.1494320249 -0.0002066200	-0.0360238122 -0.0016435355
800	0.2143746840 -0.0000028760	0.1951171158 -0.0000284475	0.1493287310 -0.0001033261	-0.0368554579 -0.0008118898
1600	0.2143732463 -0.0000014384	0.1951028945 -0.0000142262	0.1492770720 -0.0000516671	-0.0372637914 -0.0004035563
3200	0.2143725272 -0.0000007193	0.1950957821 -0.0000071137	0.1492512396 -0.0000258346	-0.0374661565 -0.0002011912
EXACT	0.2143718079	0.1950886683	0.1492254049	-0.0376673477

error using 25 increments was .000900, and the error was halved by increasing the number of increments to 50. This trend continued through the run that used 3200 increments and resulted in an error of 0.000007. It was decided that an error of 0.00002, which resulted from the use of 100 increments, was acceptable. The value of each horizontal wave number determined in subroutine 'eigens' was intended only as a starting point for the more accurate subroutines 'modes1' and 'modes2'. The accuracy, therefore, has significance only in that, if two modes are closer together than single precision accuracy limitations, there would be a chance that a mode will be missed completely.

Subroutine 'eigens' was also checked using sound speed profiles that varied linearly, both positively and negatively, with depth. Since no clear-cut means of assessing the error was available, no conclusions could be drawn, and results are published for only the positive gradient (Table 4.2a). In addition, by using a sound speed profile that produced two strong ducts, it was possible to show that 'eigens' was capable of distinguishing between two horizontal wave numbers which are very close together (Table 4.2b). The solutions are not precise but no modes are missed and the necessary information is provided to the subsequent subroutines where the values are calculated to the required precision.

Next, normalized modal pressures at a large number of depth increments were calculated using 'modes2'. These data were combined in Figure 4.1 and show, for each mode, the relative amplitude of the modal pressure function. The profiles for all three real modes as well as the first evanescent mode are plotted together and care must be taken to note that they represent the modal characteristics, not the actual

TABLE 4.2. SUBROUTINE 'EIGENS' - SQUARES OF MODAL HORIZONTAL  
WAVE NUMBERS FOR A. POSITIVE GRADIENT, AND B. DUAL  
DUCT FOR 50 HZ SOURCE AND 500 METERS DEPTH.

MODE NUM	POSITIVE GRADIENT	DOUBLE DUCT
1	0.2023466395	0.2094159684
2	0.2017806065	0.2092275382
3	0.2015439681	0.2088501680
4	0.2009845610	0.2082828312
5	0.2001803173	0.2075239702
6	0.1991866971	0.2065714750
7	0.1980052050	0.2054226531
8	0.1966276551	0.2040741897
9	0.1950384284	0.2025220985
10	0.1932226702	0.2007616580
11	0.1911713327	0.1987873347
12	0.1888803823	0.1965926865
13	0.1863476142	0.1941702449
14	0.1835693580	0.1915113682
15	0.1805375878	0.1896060596
16	0.1772381208	0.1854427397
17	0.1736509107	0.1820079592
18	0.1697523042	0.1782860324
19	0.1655174308	0.1742585647
20	0.1609207800	0.1699038333
21	0.1559344080	0.1651959631
22	0.1505243249	0.1601038096
23	0.1446458558	0.1545894076
24	0.1382386306	0.1486057637
25	0.1312213613	0.1420936161
26	0.1234851760	0.1349764974
27	0.1148818518	0.1271528691
28	0.1051995705	0.1184828654
29	0.0941103985	0.1087642801
30	0.0810451735	0.0976846549
31	0.0648246885	0.0847116344
32	0.0419336933	0.0687821079
33	-0.0276373313	0.0469792092
34	0	-0.0198930514



pressure contributions. The figure shows that, for rigid bottom, no absorption, iso-speed conditions, the profiles meet the boundary conditions at the top, where pressure is zero, and at the bottom, where the derivative is zero. The same test procedure was repeated using subroutine 'modes1' and identical results were obtained.

To illustrate the relative degree to which each mode is stimulated, depending on the depth of receiver and transmitter, a trial run was made with a transmitter at depth 13 meters and receiver at various depths. Figure 4.2 depicts the relative strength of each mode at each depth. The second mode is most strongly stimulated and mode 1 is least strongly stimulated, as could be anticipated from Figure 4.1.

Routine FFP does not use exact normal mode horizontal wave numbers, but boundary conditions must remain consistent and sinusoidal variations still occur at a rate defined by the vertical wave number,  $k_z$ , which, in turn, is a function of the horizontal wave number,  $\xi$ . The results of subroutine 'modes1' were compared to the values of  $\sin(k_z z_>)$  and the results of 'modes2' were compared to the values of  $\cos(k_z(H-z_<))$ , where  $H$  is the water depth and  $z_>$  and  $z_<$  are the depths of the receiver and transmitter. The comparisons showed that the subroutines worked properly.

At this point, the solution using calculated horizontal wave numbers in EXACT was examined for accuracy. It was decided that the accuracy criterion would be based upon the worst case which allowed for all errors to be cumulative. It can be seen in Equation 2.31 that an error in  $\xi_n$  will exhibit itself directly in the square root and in the exponential. A small error causes only a small error in the square root but it



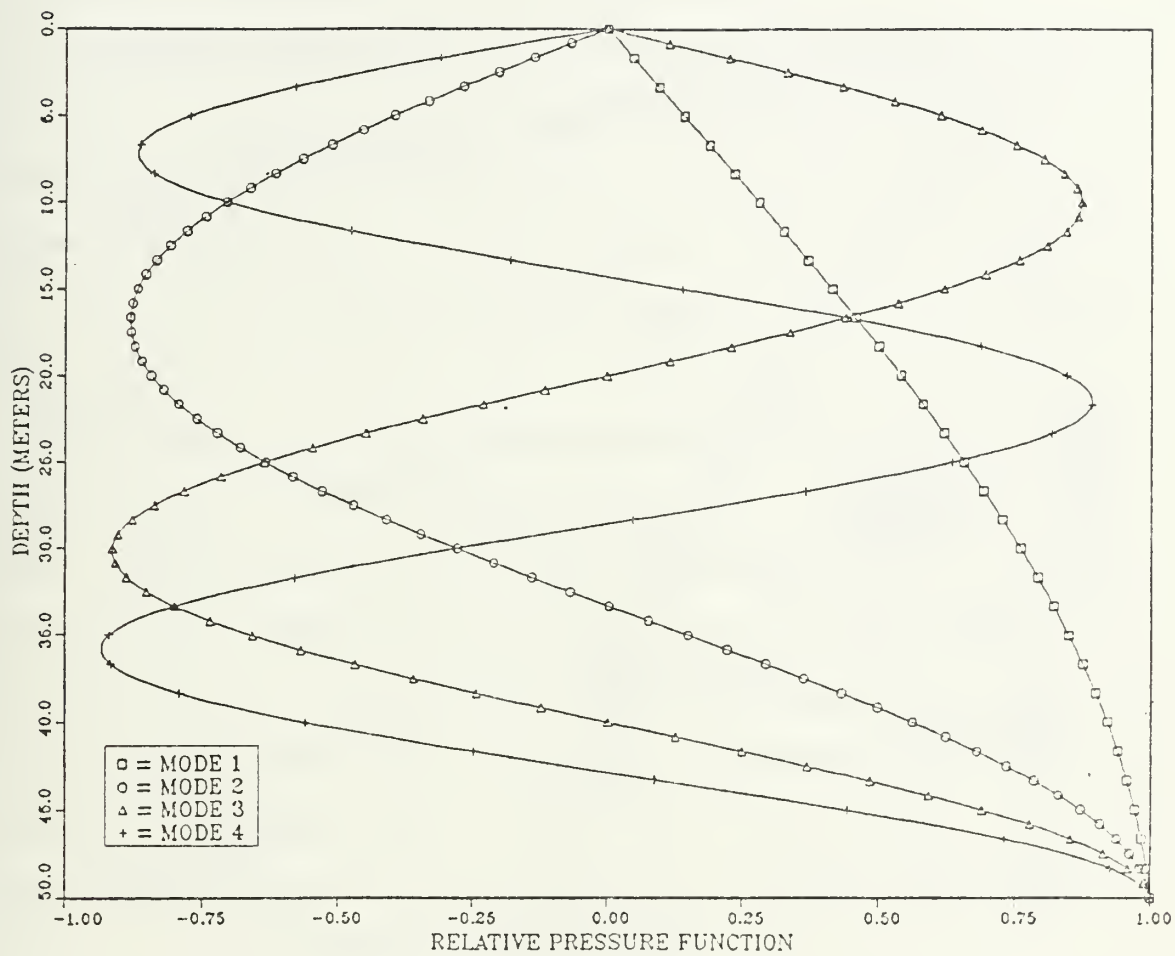


Figure 4.1. Modal Pressure Function for Three Real Modes and Evanscent Mode, Individually Normalized.

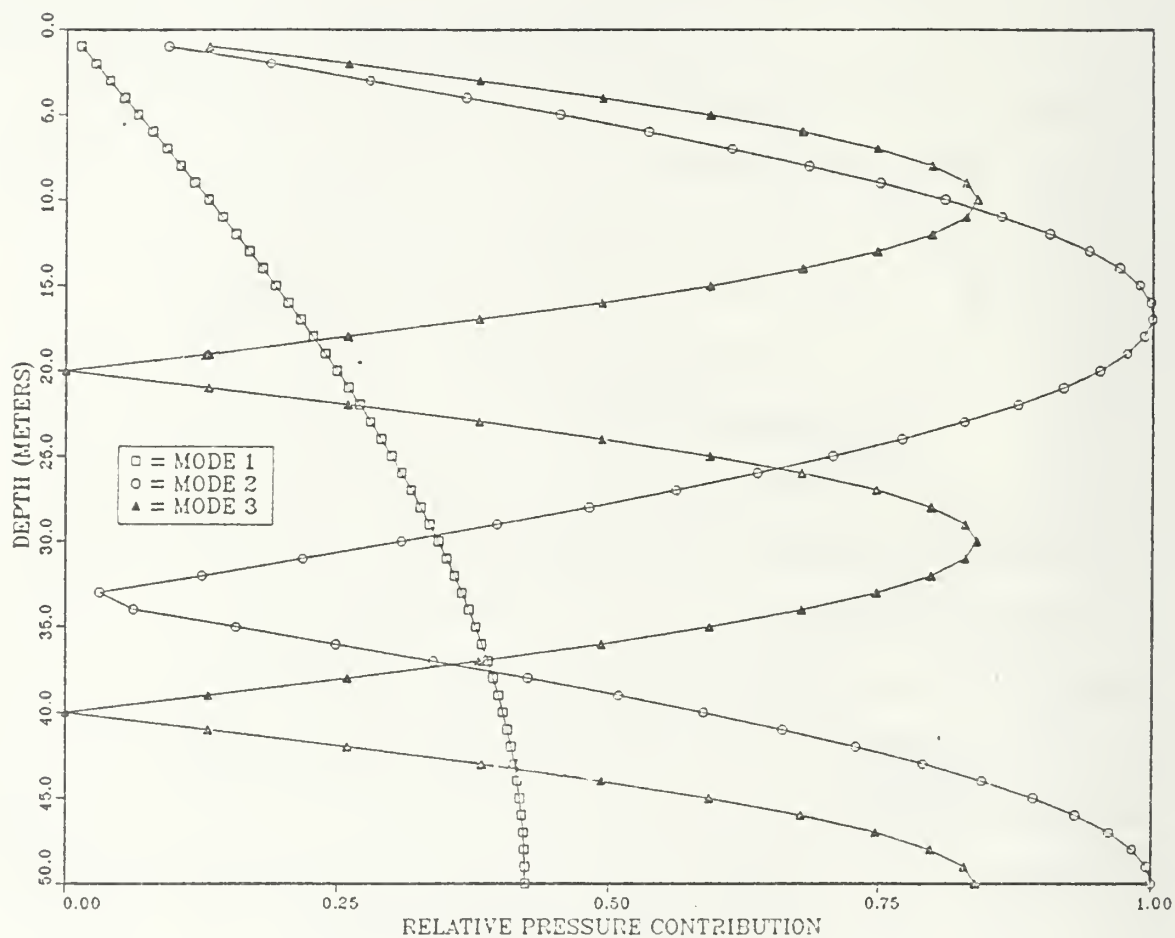


Figure 4.2. Pressure Contributions Normalized to the Maximum Value of the Most Strongly Excited Mode for Source at 13 Meters.

is critical in the phase component. It was categorically decided that the maximum allowable phase error for each mode would be 0.1 radians, and that the maximum range would be 100,000 meters. This limits the maximum error in  $\xi_n$  to  $10^{-6}$  for all wave numbers..

In assessing possible real errors, a vector plot was made for each of several solutions. A constant adjustment was then introduced to each of the horizontal wave numbers, giving them an artificial error. It can be seen in Figure 4.3 that for short ranges, a large error is admissible and, even at 50,000 meters, the limit imposed by the accuracy criterion is well within the allowable error.

Vector plots were also used to illustrate how a small change of range can cause a dramatic change in pressure. Figure 4.4a shows the change of propagation loss from 830 to 840 meters. Most of the change is involved with phase and the amplitude change is small. This can be seen best in Figure 4.4b where the range change is only one meter. It should be noted too, that these errors have been made cumulative whereas it is unlikely that the errors would ever be that way. One would therefore expect the total error to be less than that illustrated.

A plot of loss with range for a rigid bottom, Figure 4.5, showed a general  $20 \log R$  increase in propagation loss close to the source and a change of  $10 \log R$  as the distance increased. Superimposed on this is a strong interference pattern from the three real modes. Sudden changes of pressure with changing range, as were noted in Figure 4.4, are seen as rapid fluctuations or propagation loss in this plot. A decisive check on the general reliability of the program to this point involved excluding

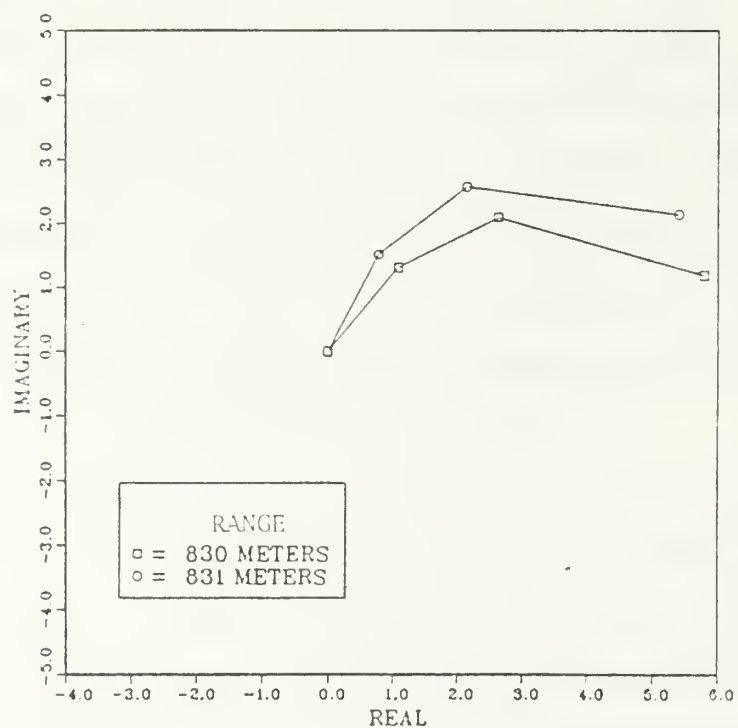
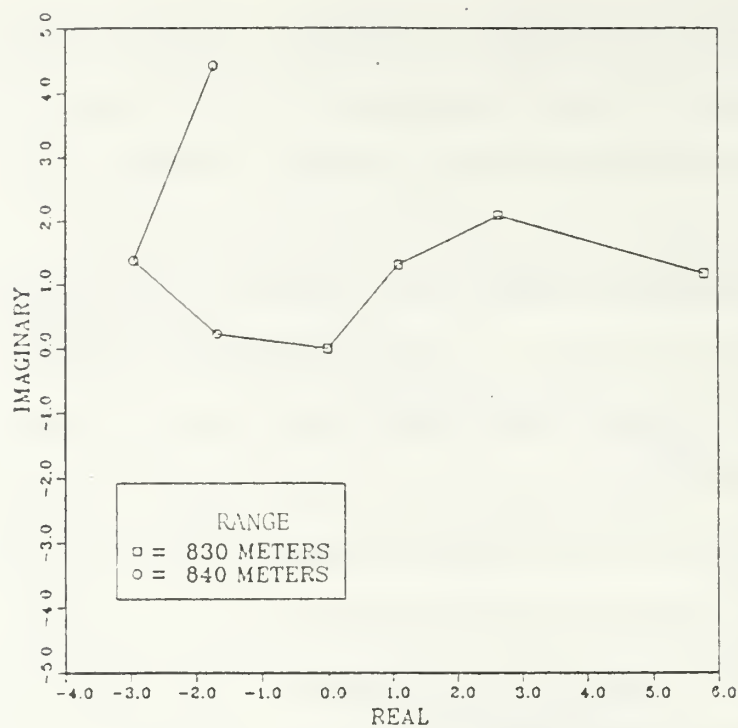


Figure 4.3. Pressure Components for Three Real Modes Illustrating Cumulative Error from Errors in Horizontal Wave Number at 50 Meters (Upper) and 50 Km (Lower).

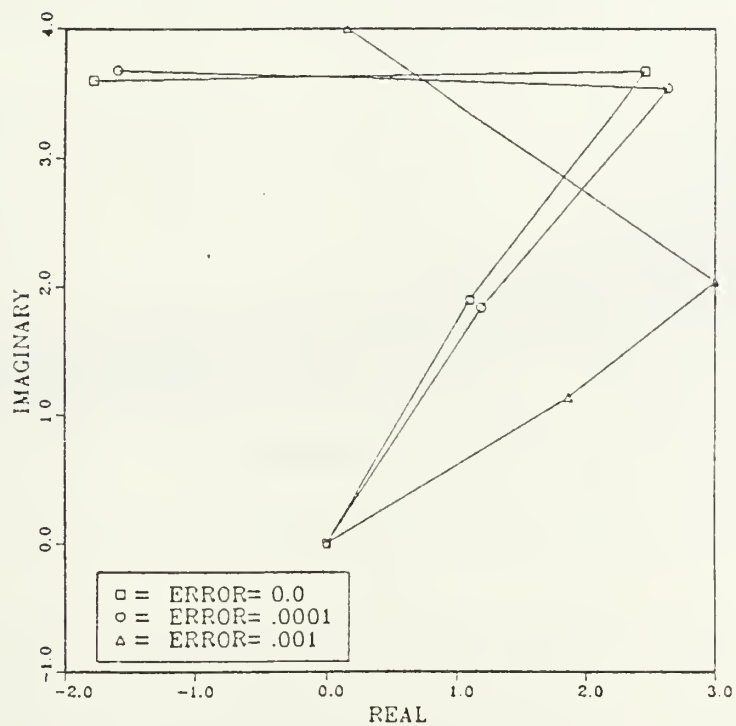
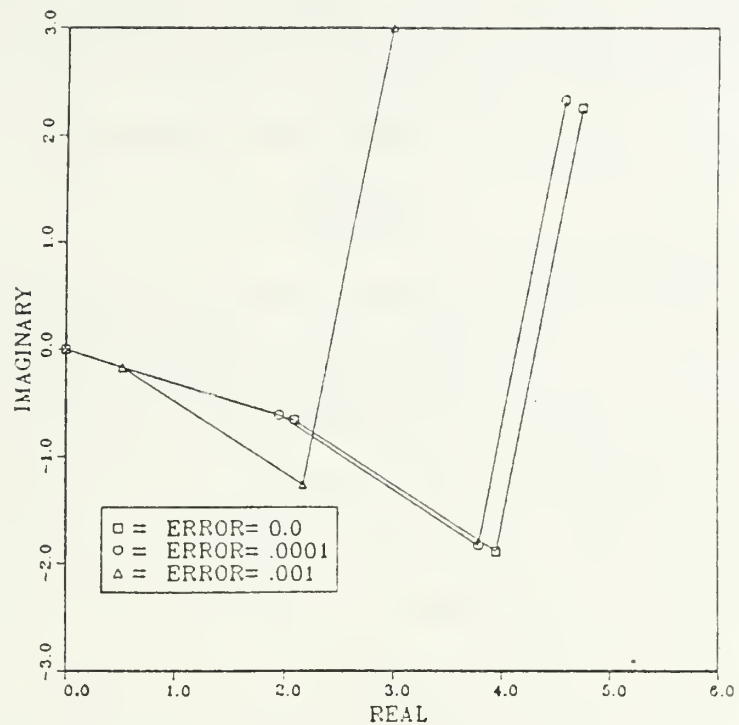


Figure 4.4. Components of Pressure illustrating Sudden Changes of Pressure with Range.

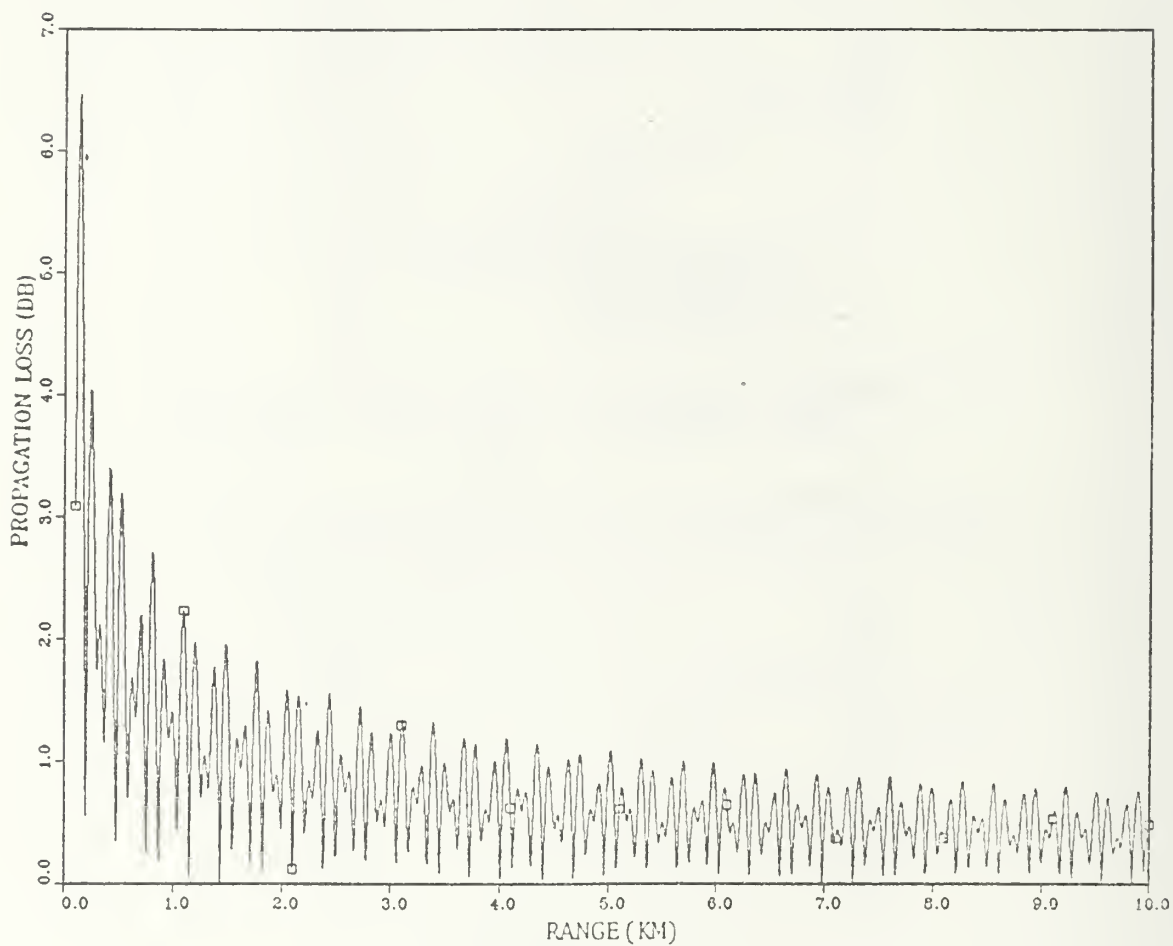


Figure 4.5. Propagation Loss for Source at 10 Meter Depth and Receiver at 37 Meters in 50 Meter Ocean.

all but two real modes and plotting the resulting propagation loss curves. For each pair of modes, the interference distance can be shown to be related to the horizontal wave numbers by:

$$R = \frac{2\pi}{\xi_m - \xi_n} \quad 4.2$$

where:

R is the horizontal distance between nulls,

and  $\xi_m$  and  $\xi_n$  are the real horizontal wave numbers.

Comparison was made between the calculated interference distance and the observed distance for all three interference combinations and proved to be correct in all cases. Figure 4.6 shows the result when the first and third modes were used. The cycle distance was calculated to be 96.5 meters, which agrees with the distance from the plot.

#### B. RIGID BOTTOM WITH ABSORPTION

Absorption due to water (low frequency), although normally very small, was made artificially high to check on the mechanics of the program. With absorption set to an arbitrary value of 0.0005 nepers/meter, it was noted that the imaginary component of the wave number increased with the increasing grazing angle associated with higher modes: 0.000505 for mode 1, 0.000555 for mode 2, and 0.000727 for mode 3.

To ensure that output losses were consistent with those input, other propagation loss curves were drawn using a variety of rates of absorption. Figure 4.7 shows that the difference in loss at any given range is 8.7 times the difference of absorption rates (as expected from Equation 2.42). For example, a change from 0.0000001 nepers/meter to 0.0001



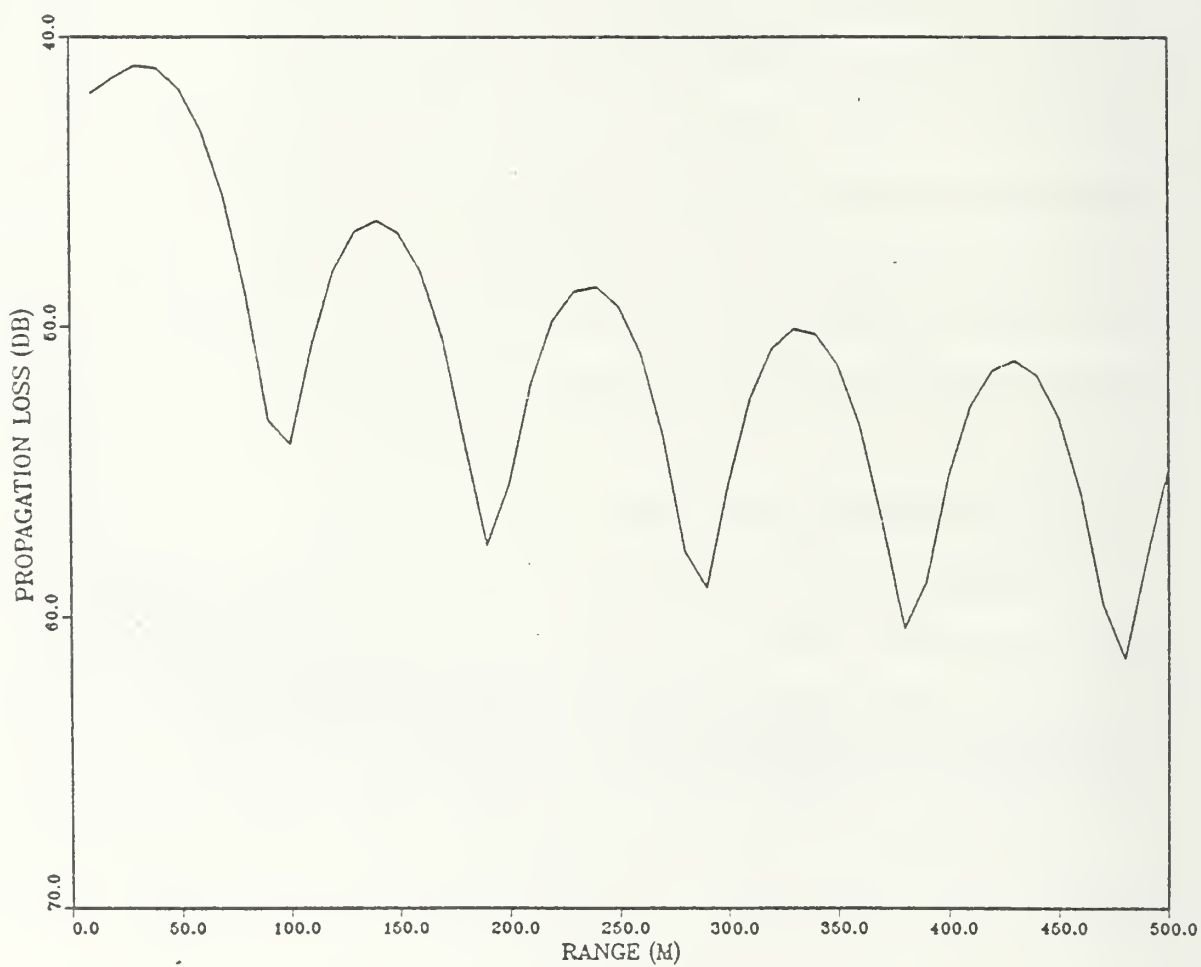


Figure 4.6. Interference Pattern Between Modes 1 and 3 for Source at 10 Meters and Receiver at 37 Meters in 50 Meters of Water for 50 Hz.

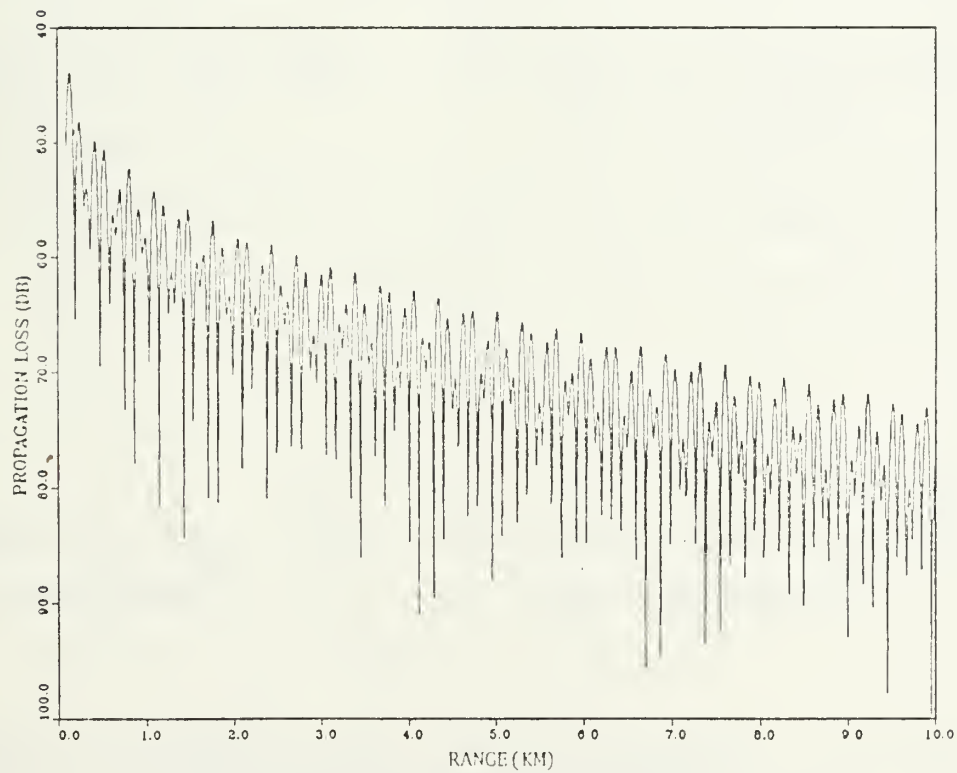
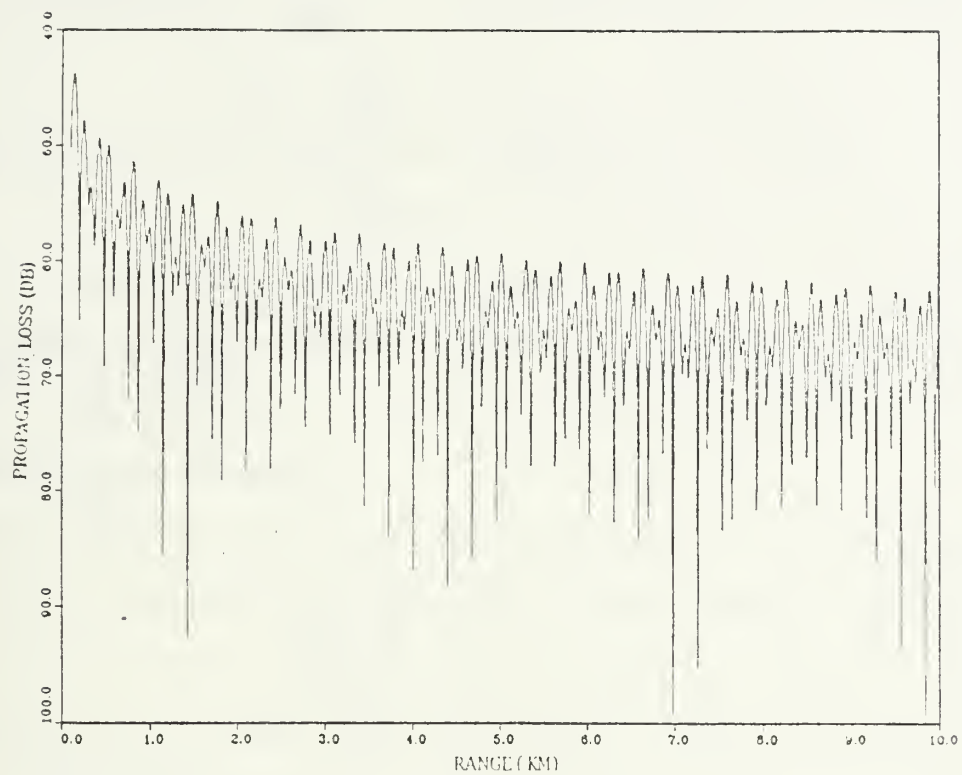


Figure 4.7. Propagation Loss for Absorption Rate 0.000001 Nepers/Meter (Upper) and 0.0001 Nepers/Meter (Lower).

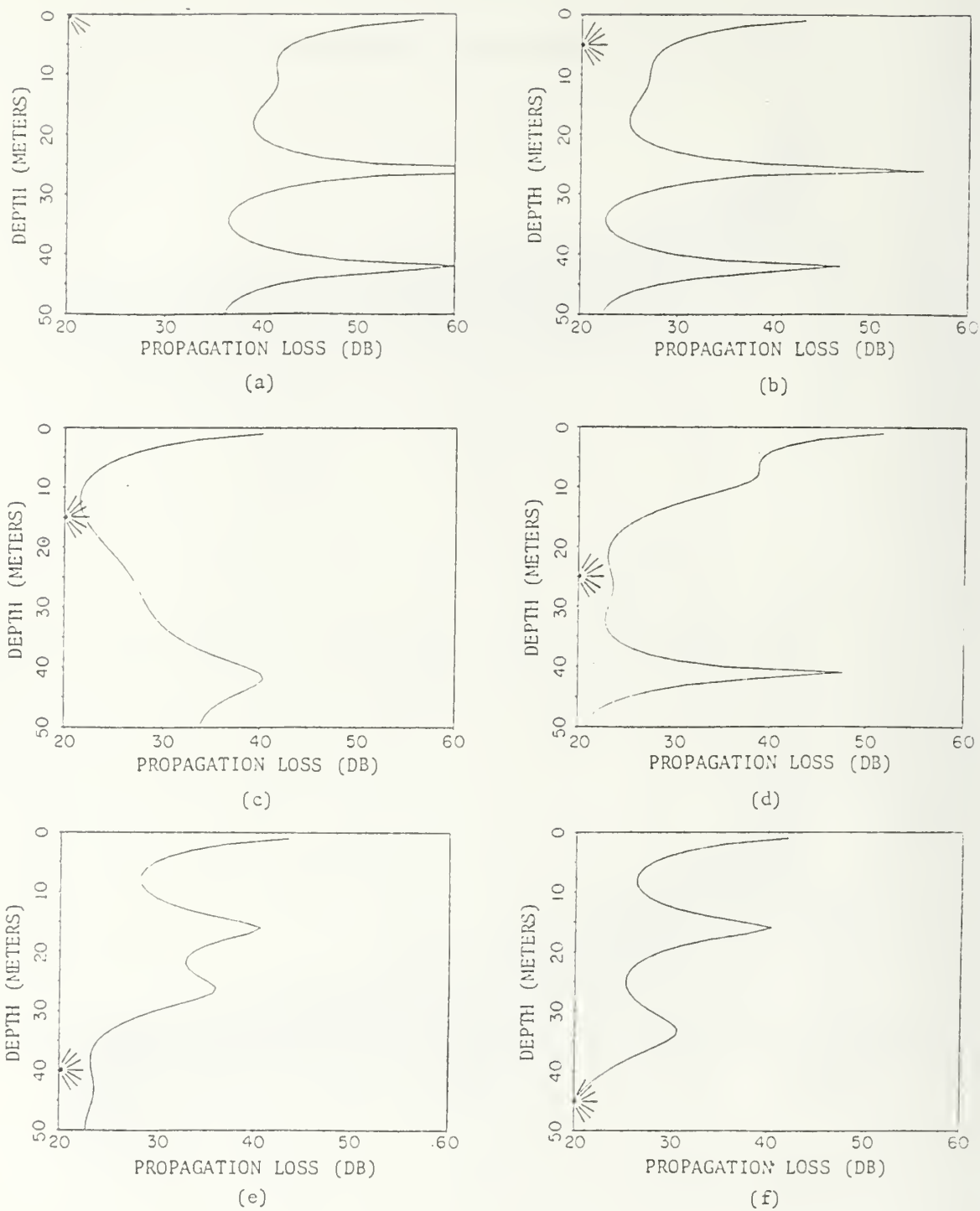


Figure 4.8. Propagation Loss as a Function of Depth for Sources at:  
a. 1 Meter, b. 5 Meters, c. 15 Meters, d. 25 Meters,  
e. 40 Meters, and f. 45 Meters.

neper/meter causes a change of propagation loss, at 10 kilometers, of 9.0 dB. One would have expected a change of 1.0 neper or 8.7 dB.

A series of runs was made to illustrate how pressure varies with receiver depth at a set range for a variety of source depths. From the graphs (Figure 4.8) it is important to note that for a source or a receiver at the surface, the pressure will be zero and the propagation loss infinite because none of the modes is stimulated. This does not change when an impedance bottom is introduced, but it would change if a real surface were considered.

Using these same depth profiles, it was possible to further verify the program by checking for reciprocity. The propagation loss is, for example, the same for a combination of a source at 5 meters and receiver at 25 meters as for a source at 25 meters and receiver at 5 meters.

The final set of tests for a rigid bottom involved the use of the FFP. At the point of testing, the Fourier transform (FFT) had not yet been introduced so pressure factors were being calculated for individual ranges. Figure 4.9 shows that, for a zero absorption loss, the only horizontal wave numbers that contribute to the total are at the exact mode values. Small changes of the horizontal wave number cause serious changes in the value close to the exact mode value.

Introduction of absorption causes the energy to be dispersed across the spectrum. There are small contributions from across the wave number spectrum and flattening at the modes. Higher absorption causes greater dispersion of the 'pressure'. The integral, with absorption, can be seen to fluctuate in Figure 4.10, staying close to zero until the first mode is approached. The integral increases quickly, but not

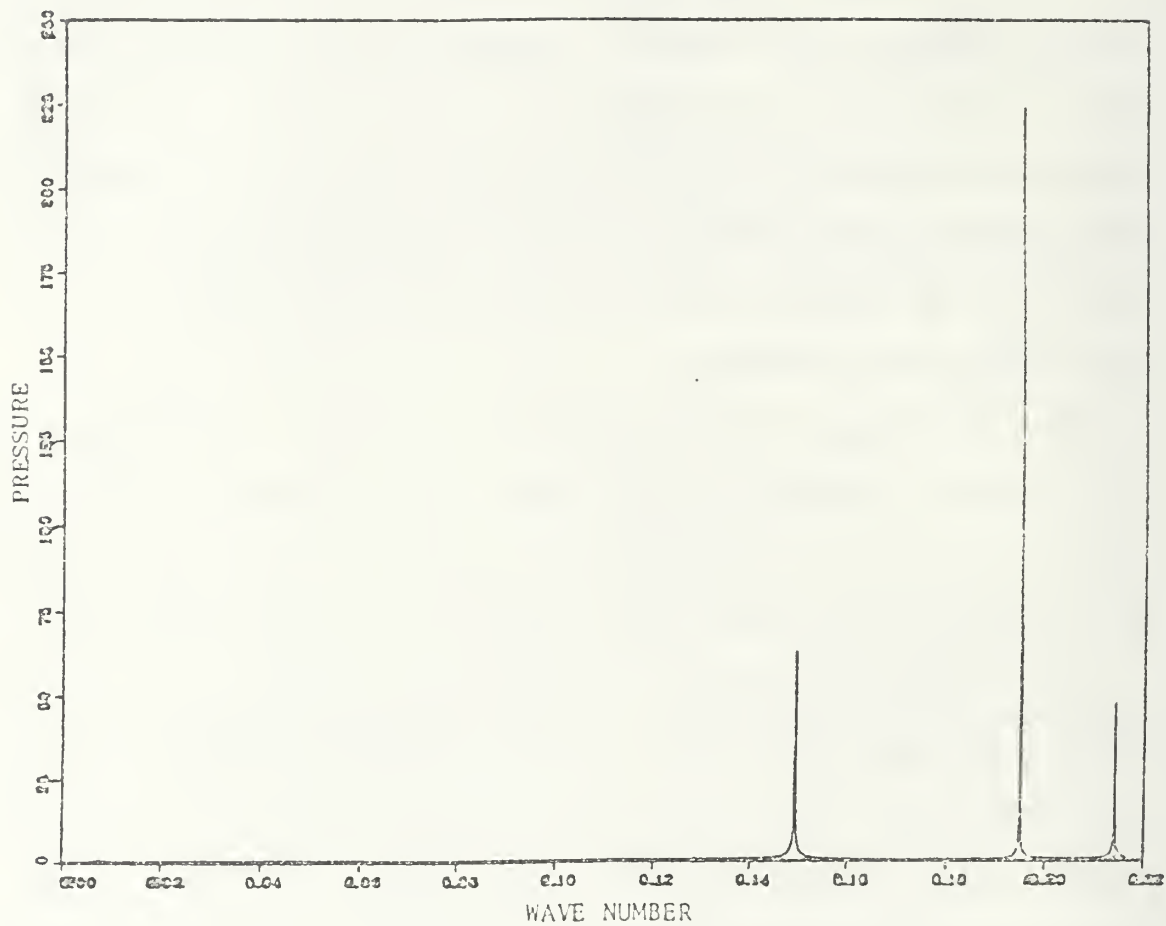


Figure 4.9. Amplitude of Sound Pressure Factor for Individual Wave Numbers with No Absorption.

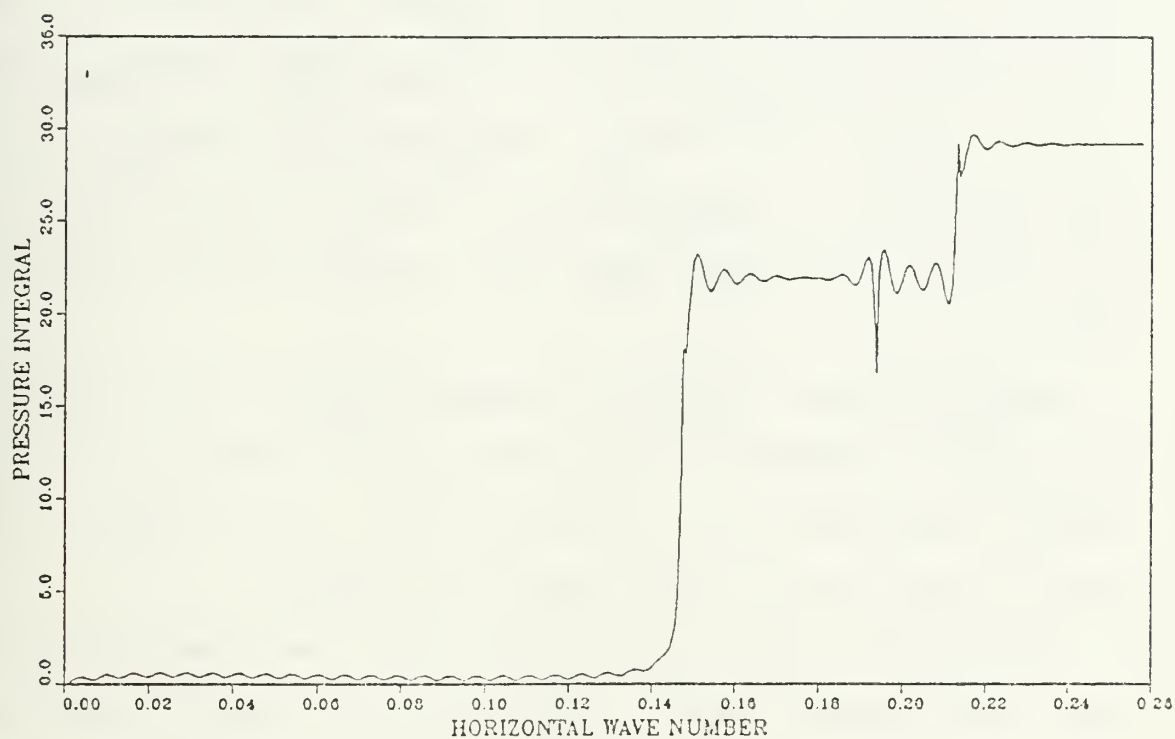


Figure 4.10. Integrated Pressure with Absorption Rate  
 0.00005 Nepers/Meter at Range 10000 Meters,  
 Tx/Rx at 10/37 Meters, 50 Meter Ocean, 50 Hz.

abruptly when a mode is reached. A sharp decline is notable when the 180 degree phase change occurs at the mode. The final value represents the final pressure at the receiver.

Various checks were made to ensure proper functioning of the FFP program for a given range. By changing the number of wave number increments, it was found that the maximum amplitude for each mode changed (Figure 4.11) but that the integrated pressure was identical when the number of increments was changed from 1024 to 2048. Pressures agreed with one another to the seventh decimal and fifth significant digit. Given more time, it would have been interesting to see how few samples could be taken, for a single range, before significant errors were introduced.

Figure 4.12 shows the effect of changing absorption rates. However, the change of pressure at a given range does not correlate with the change of absorption rate. This indicated that the FFP routine was incorrect in some way and further checks were required.

The integrated pressures from this program were then compared to the values obtained from the program EXACT for different absorption rates and ranges. As can be seen in Table 4.3, agreement was poor. Because of time constraints, it was decided to abandon the FFP and concentrate on solutions using the EXACT method.

NOTE: A great deal of time had been spent on FFP trying to find a solution for a fixed range, a prerequisite to implementation of the 'FFP' subroutine. At the time that work with the FFT was first suspended, it gave inconsistent results that did not meet any of the testing criteria. A small change of increment size, from 2047 to 2048 increments, caused

TABLE 4.3. CALCULATED PRESSURE FOR PROGRAM FFP AND EXACT.

RANGE (METERS)	ABSORPTION (NEPERS/METER)	PRESSURE FACTOR	
		FFP	EXACT
1000	0.0000001	0.00172867	0.00139872
1000	0.00001	0.00128178	0.00138953
2000	0.0000001	0.00001486	0.00139504
2000	0.00001	0.00010503	0.00138101



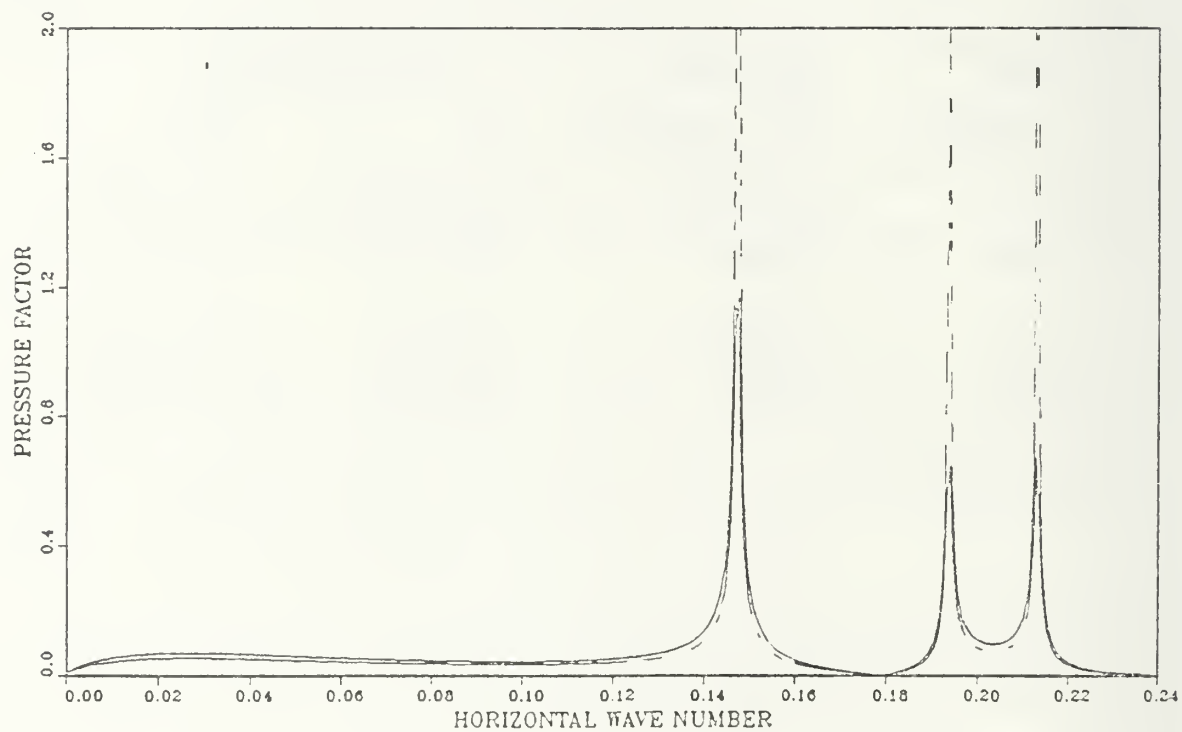


Figure 4.11. Amplitude of Sound Pressure for Absorption  
0.0005 Nepers/Meter Using: 1024 Wavenumber  
Samples (Dashed Curve) and 2048 Samples (Solid.)

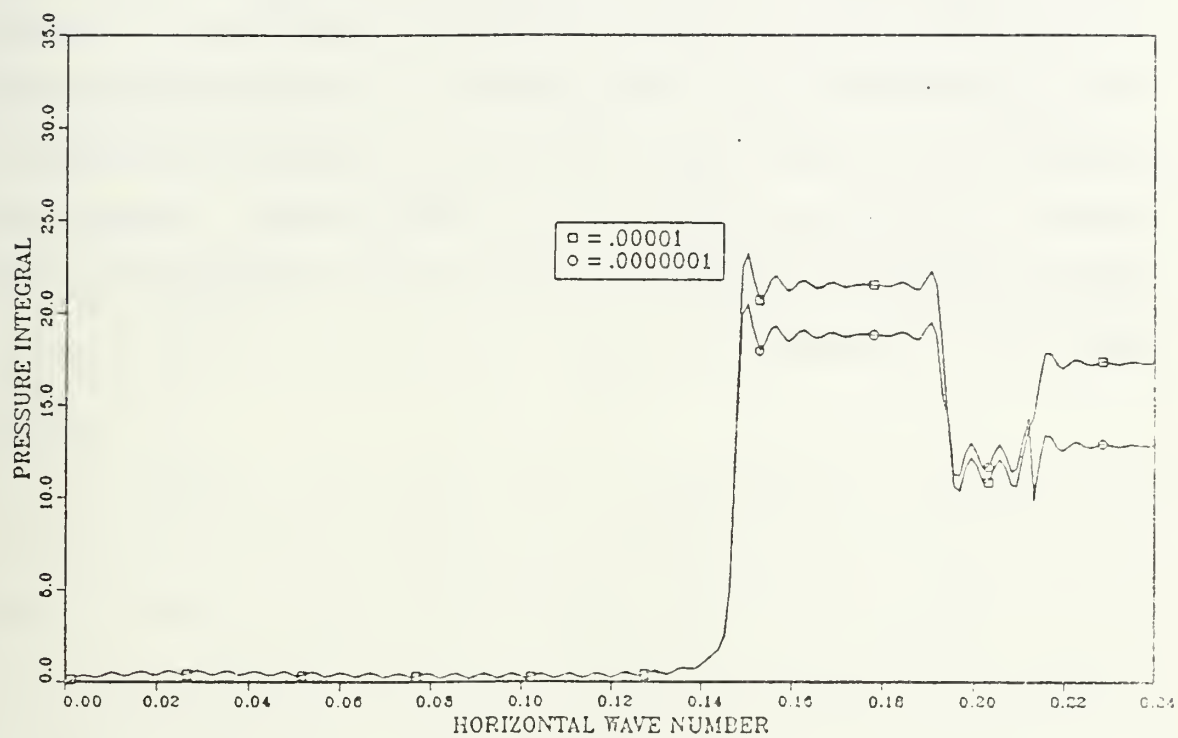


Figure 4.12. Integrated Pressure for Absorption Rate  
 a. 0.00001 Nepers/Meter (Lower) and  
 b. 0.0000001 Nepers/Meter (Upper) Range 1000 Meters.

outlandish changes in the integrated pressure. The changes of pressure resulting from a changed absorption rate did not correspond, even remotely, with the changes expected. At that point, priorities were shifted and it was decided to concentrate on solving the 'EXACT' program problems at the expense of the 'FFP'. At a later date, too late to be practically helpful, some of the FFP problems were rectified and the above mentioned inconsistencies were remedied. It was possible to relate propagation loss to absorption rate and it was shown that the number of samples has a negligible effect on the final pressure. However, the discrepancy between the EXACT solution and the FFP solutions still exist and the FFP is incomplete.

### C. IMPEDANCE BOTTOM

The introduction of an impedance bottom to replace the perfectly reflecting rigid bottom made it possible to better predict the propagation loss experienced in reality. This was done by defining the bottom in terms of its density and the sound speed in the bottom at the interface. After continued failure of the program to solve for modes whose grazing angles were far below the critical angle and the eventual resolution of that problem, a series of tests was devised to try to optimize the program. These tests also provided a convenient means of illustrating how various angles of incidence associated with the different modes resulted in the varying phase changes and amplitudes of reflected energy.

As with the rigid bottom case, it was possible to plot the modal pressure as a function of depth, from the reflecting surface to the impedance bottom. Figure 4.13 shows how the pressure reaches a maximum well above the bottom for mode 1. The grazing angle, in this case, is less than the critical angle and illustrates the phase advance at the bottom. The test was repeated for strong positive and negative gradients but showed little change.

The first set of tests to check on final accuracy involved using a critical angle of 0.3 radians and was intended to find the optimal number of increments. It had been determined earlier that accuracy to the ninth decimal, or better, was obtainable (iso-speed) for all modes using 200 depth increments/mode. At 100, the accuracy dropped to the seventh decimal and at 50, answers were accurate to only the fourth

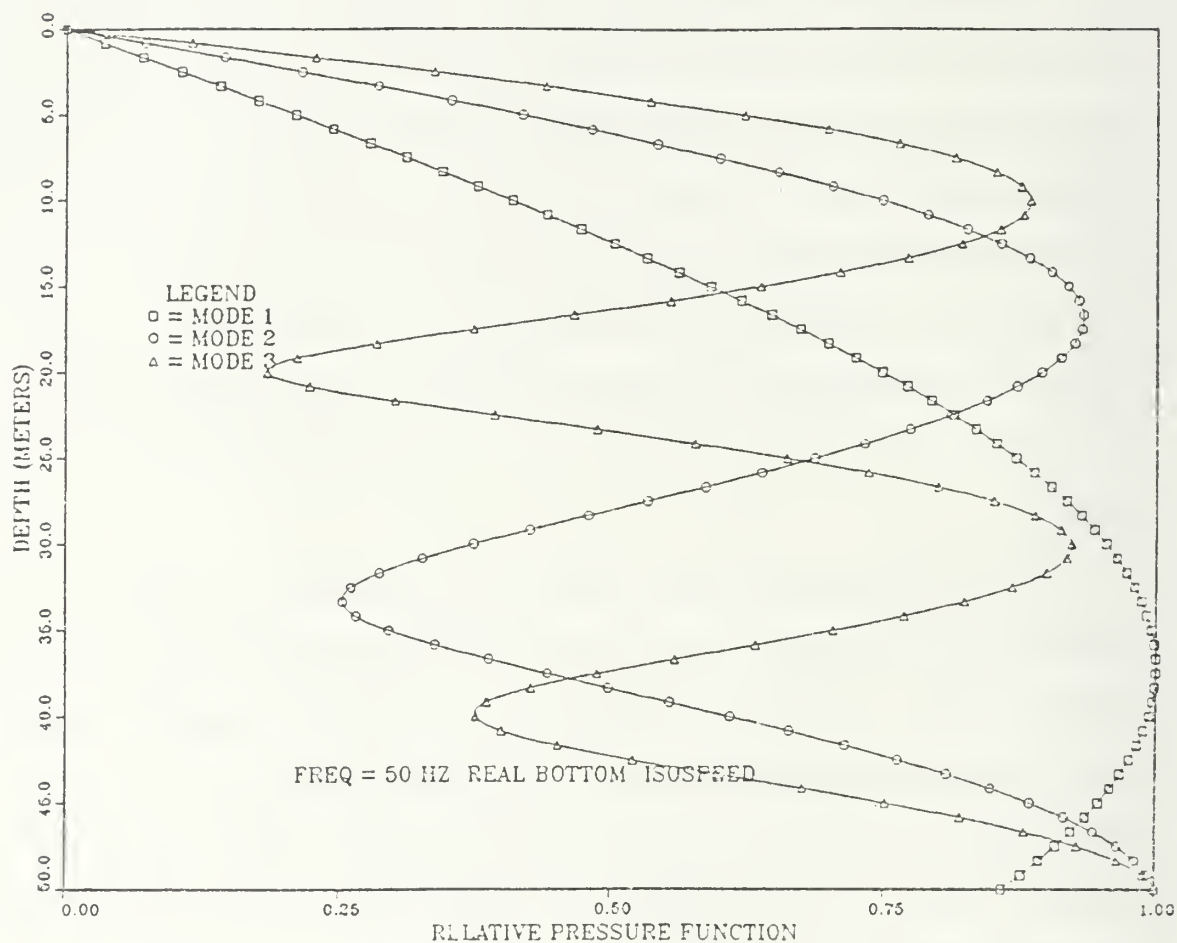


Figure 4.13. Relative Pressure Function for 3 Real Modes for Critical Angle 0.3 Radians, Isospeed Water Conditions, 50 Hz Source.

decimal. Table 4.4 shows horizontal wave numbers that were calculated using 100, 200, 400 and 600 depth increments/mode in combination with correction factors of 1, 2, 5 and 10. The correction factor was divided into the mode wave number correction term of subroutines 'modes1' and 'modes2' to limit the size correction and thus prevent instability. These correction factors were found necessary for modes whose grazing angles were less than the critical angle (in this case only mode 1). Without a correction factor, the program would fail to converge to an acceptable solution but would become divergent.

A major problem in deciding the best choice of variables came about because there was no correct answer against which to appraise the values. It was reasoned that 800 increments per mode and a correction factor of 10 would give the most accurate answer and the problem narrowed down to finding a combination that gave an acceptable accuracy with a reasonable number of iterations. Having decided that 200 increments/mode was sufficient and necessary for the rigid bottom case, it became a question of how large the correction factor could be. The choice was further narrowed to a correction factor of 2 with an error of  $9.8 \times 10^{-8}$  and 40 iterations required and a factor of 5 with an error of  $3 \times 10^{-8}$  and 89 iterations. Because the error was borderline for the correction factor 2, the final choice was 200 intervals/mode with a correction factor of 5.

Using the inputs as decided above, an effort was made to correlate actual accuracy with that specified as a requirement. Results for trials on all modes using accuracy criteria from  $10^{-5}$  to  $10^{-13}$  follow in

TABLE 4.4. PROGRAM 'EXACT' - REAL AND IMAGINARY COMPONENTS OF  $\xi^2$   
FOR MODES 1 TO 4 RESULTING FROM VARIATION OF NUMBER  
OF DEPTH INCREMENTS AND 'CORRECTION' FACTORS.

COR INC ITER	1	2	3	4
1 100 90	0.212512884 0.000450164	0.195507949 -0.003339831	0.150035436 -0.010172100	0.002867414 0.037779947
2 100 38	0.212512965 0.000450172	0.195507949 -0.003339831	0.150035436 -0.010172100	0.002867414 0.037779947
5 100 89	0.212513034 0.000450172	0.195507949 -0.003339831	0.150035436 -0.010172100	0.002867414 0.037779947
10 100 185	0.212513060 0.000450170	0.195507949 -0.003339831	0.150035436 -0.010172100	0.002867414 0.037779947
1 200 74	0.212512885 0.000450165	0.195507947 -0.003339830	0.150035443 -0.010172094	0.002867435 0.037779660
2 200 40	0.212512968 0.000450171	0.195507947 -0.003339830	0.150035443 -0.010172094	0.002867435 0.037779660
5 200 89	0.212513036 0.000450172	0.195507947 -0.003339830	0.150035443 -0.010172094	0.002867435 0.037779660
10 200 185	0.212513063 0.000450170	0.195507947 -0.003339830	0.150035443 -0.010172094	0.002867435 0.037779660
1 400 67	0.212512885 0.000450165	0.195507946 -0.003339830	0.150035443 -0.010172093	0.002867437 0.037779642
2 400 40	0.212512969 0.000450171	0.195507946 -0.003339830	0.150035443 -0.010172093	0.002867437 0.037779642
5 400 89	0.212513038 0.000450172	0.195507946 -0.003339830	0.150035443 -0.010172093	0.002867437 0.037779642
10 400 185	0.212513065 0.000450170	0.195507946 -0.003339830	0.150035443 -0.010172093	0.002867437 0.037779642
1 800 72	0.212512885 0.000450165	0.195507946 -0.003339830	0.150035443 -0.010172092	0.002867437 0.037779641
2 800 39	0.212512969 0.000450171	0.195507946 -0.003339830	0.150035443 -0.010172092	0.002867437 0.037779641
5 800 90	0.212513039 0.000450171	0.195507946 -0.003339830	0.150035443 -0.010172092	0.002867437 0.037779641
10 800 187	0.212513066 0.000450170	0.195507946 -0.003339830	0.150035443 -0.010172092	0.002867437 0.037779641
EXACT (RIGID BOTT)	0.214371820 0.000505340	0.195088818 0.000555289	0.149226333 0.000725949	0.002867437 0.037779640



Table 4.5. Assuming that the answers obtained using  $10^{-13}$  had the least error and could then serve as a standard, errors were calculated as the difference between the standard and each answer. It was found, in all cases, that the actual errors were slightly less than those specified by the accuracy criteria. This was to be expected since corrections were made to make the error less than the designated amount.

The final check involved the problems associated with low modes whose grazing angles were less than the critical angle. A series of calculations was made to find the number of iterations required for different critical angles (different sound speed ratios) using a 100 meter deep, isovelocity ocean that supported seven real modes. It was also intended to uncover further problems associated with large critical angles. At the same time, the squared values of horizontal wave numbers for the seven modes were calculated for each critical angle and are shown in Table 4.6. For angles close to the grazing angle for the first mode, 0.1 radians, the program failed using both subroutines 'modes1' and 'modes2' during these runs. This was unusual because previous data had been collected for almost identical conditions.

The fraction of energy reflected and the phase change represented by the Rayleigh coefficient, were calculated for each mode for each critical angle and are shown in Figure 4.14 and 4.15 (upper). The graphs show that the loss per bounce is zero when the grazing angle is less than the critical angle. Mode 1 has the lowest grazing angle and it can be seen that the critical angle must be very low if the low modes are to suffer any attenuation at all. Higher modes suffer higher losses. To show the

TABLE 4.5. PROGRAMS 'EXACT' - REAL AND IMAGINARY COMPONENTS OF  $\xi^2$   
AND NUMBER OF ITERATIONS TO MEET REQUISITE ACCURACY.

MODE NUMBER				
ACC	1	2	3	4
	REAL IMAG ITERATIONS	REAL IMAG ITERATIONS	REAL IMAG ITERATIONS	REAL IMAG ITERATIONS
E-5	0.212519578303 0.000446662283 18	0.195507093057 0.003339285283 6	0.150034762633 0.010169974314 5	0.002867471359 0.037779636753 3
E-7	0.212512933248 0.000450155917 31	0.195507946339 0.003339829696 8	0.150035442823 0.010172092819 7	0.002867437052 0.037779642325 4
E-8	0.212512891707 0.000450175339 38	0.195507928776 0.003339803692 9	0.150035443418 0.010172073562 8	0.002867437052 0.037779642325 4
E-9	0.212512888681 0.000450176659 44	0.195507928795 0.003339804619 11	0.150035441633 0.010172073282 9	0.002867437109 0.037779642316 5
E-10	0.212512888032 0.000450176927 51	0.195507928955 0.003339804648 12	0.150035441587 0.010172073444 10	0.002867437109 0.037779642316 5
E-12	0.212512887979 0.000450176947 58	0.195507928962 0.003339804619 14	0.150035441601 0.010172073451 11	0.002867437109 0.037779642316 5
E-13	0.212512887974 0.000450176949 70	0.195507928961 0.003339804620 16	0.150035441602 0.010172073449 13	0.002867437109 0.037779642316 6

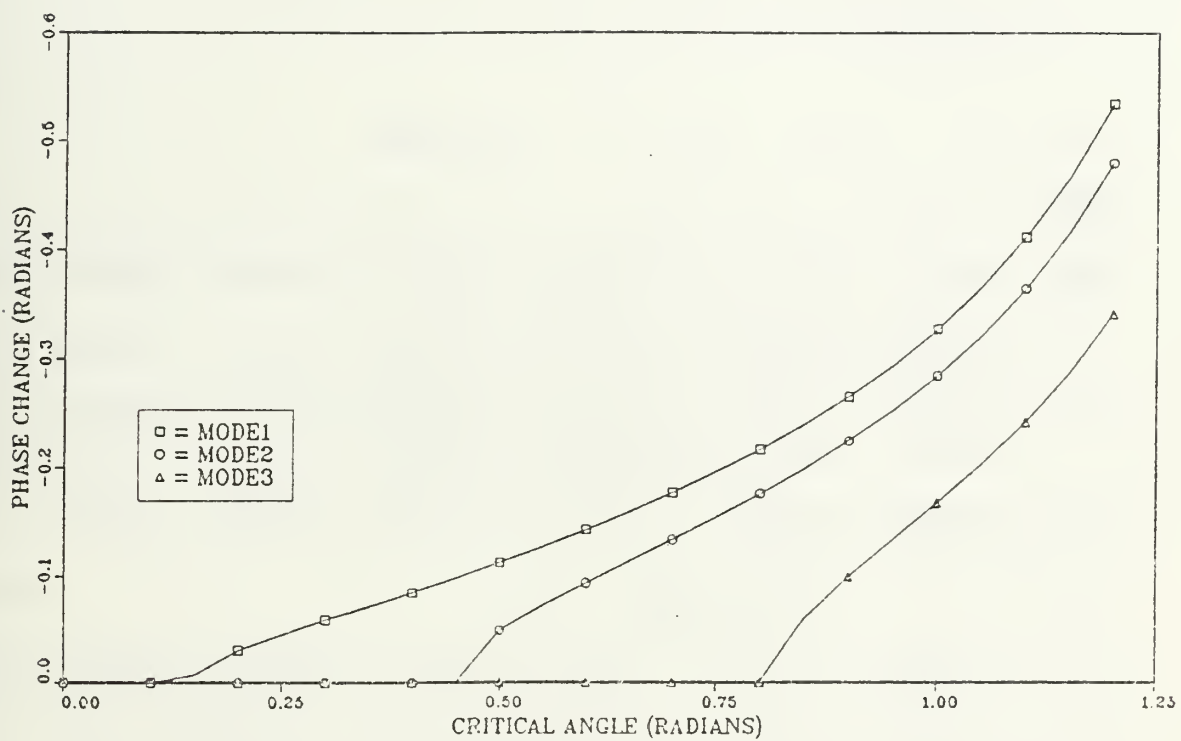


Figure 4.14. Phase Change/Bounce for 3 Real Modes as a Function of Critical Angle.

TABLE 4.6. PROGRAM 'EXACT' - REAL AND IMAGINARY COMPONENTS OF  $\xi^2$  FOR IMPEDANCE BOTTOM AS A FUNCTION OF CRITICAL ANGLE (0 TO .25 RADIANS).

CRIT ANGLE	MODE NUMBER						
	1	2	3	4	5	6	7
RIG	0.214751	0.210105	0.200490	0.185134	0.162416	0.128489	0.068307
BOT	0.000000	0.000000	0.000000	0.000000	0.000000	0.000000	0.000000
.25	0.209622	-0.209622	0.200611	0.185266	0.162595	0.128830	0.070372
	-0.000004	-0.000004	-0.001557	-0.002882	-0.004518	-0.007198	-0.015854
.20	0.210226	0.210226	0.200600	0.185258	0.162589	0.128825	0.070365
	-0.000471	-0.000471	-0.001785	-0.003022	-0.004612	-0.007258	-0.015882
.15	0.214297	0.210212	0.200591	0.185252	0.162584	0.128821	0.070360
	-0.000004	-0.000863	-0.001949	-0.003126	-0.004682	-0.007303	-0.015902
.10	UNAVAILABLE						
	UNAVAILABLE						
.05	0.213628	0.213628	0.198860	0.185216	0.162580	0.128792	0.070067
	-0.000499	-0.000499	-0.000504	-0.000591	-0.002909	-0.005782	-0.014147
0.0	0.214649	0.210107	0.200526	0.185199	0.162529	0.128739	0.069990
	-0.000123	-0.000712	-0.001612	-0.002578	-0.004114	-0.006535	-0.014437

extreme modal dependence of attenuation, Figure 4.15 (lower) displays the loss per meter for each mode for a variety of critical angles. These curves illustrate that the increased grazing angles associated with the higher modes result, not only in higher loss per bounce, but also in an increased number of bounces. For a small critical angle, say 0.1 radians, the loss per bounce is approximately three times as great for mode 2 as for mode 1, but the loss per meter is about ten times as great (Figure 4.15).

It was found that a change of critical angle (change of the sound speed ratio) changes the loss greatly. Figure 4.16 demonstrates the change of pressure due to mode 1 when the critical angle is changed from above to below the grazing angle. Changing the impedance ratio by ten per cent caused a corresponding increase in the loss but did not change the point at which the critical angle became effective.

To study the bottom loss effects for grazing angles greater than critical, different runs were made for critical angles that allowed a different number of modes to propagate in the low loss manner (grazing angle less than critical angle). Figures 4.17 and 4.18 show how much each mode contributes toward the total pressure, depending primarily upon whether its grazing angle is above or below the critical angle. They show that for each mode, when the grazing angle is less than the critical angle, the propagation loss for that mode is identical to that for the rigid bottom case.

As a last demonstration of the effects of the impedance bottom on propagation, data were compared for the isovelocity case and the strong

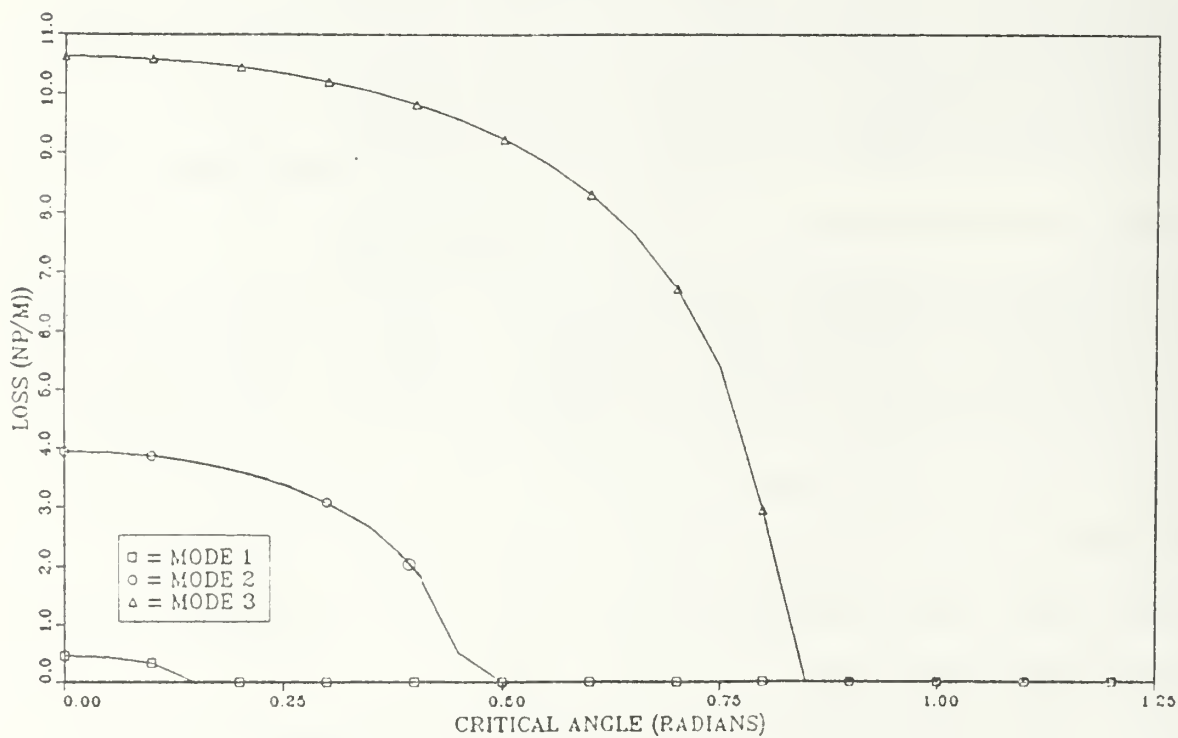
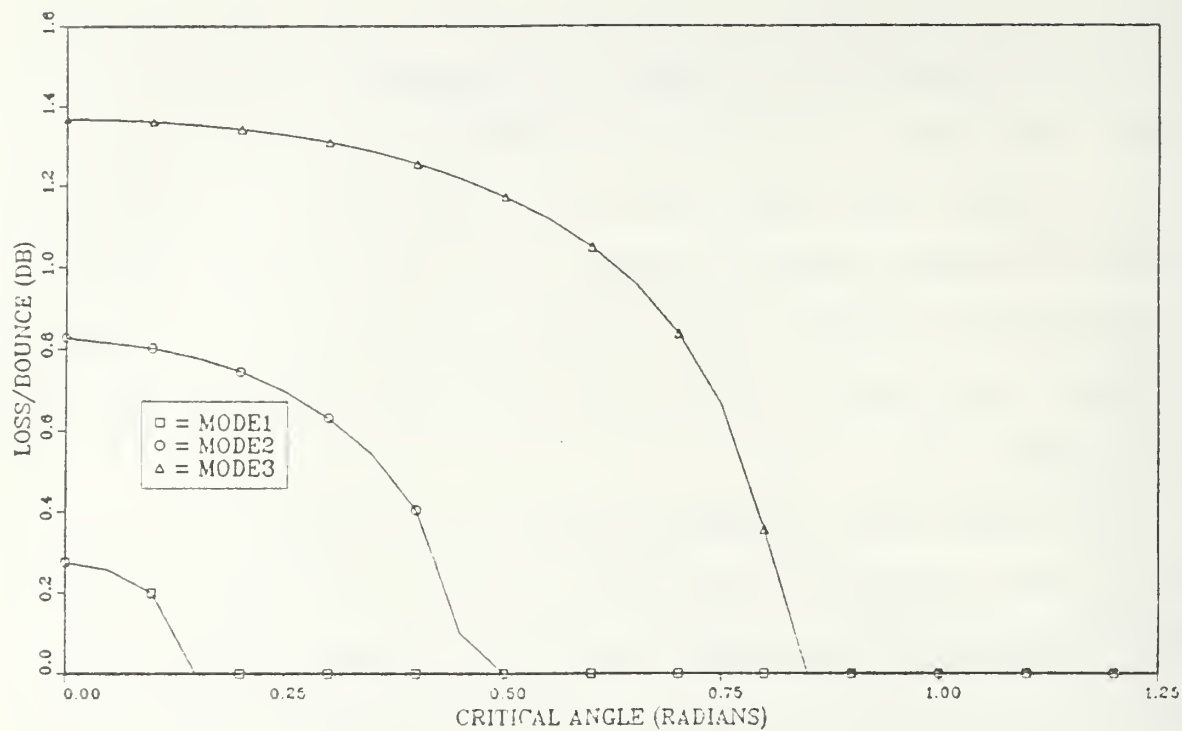
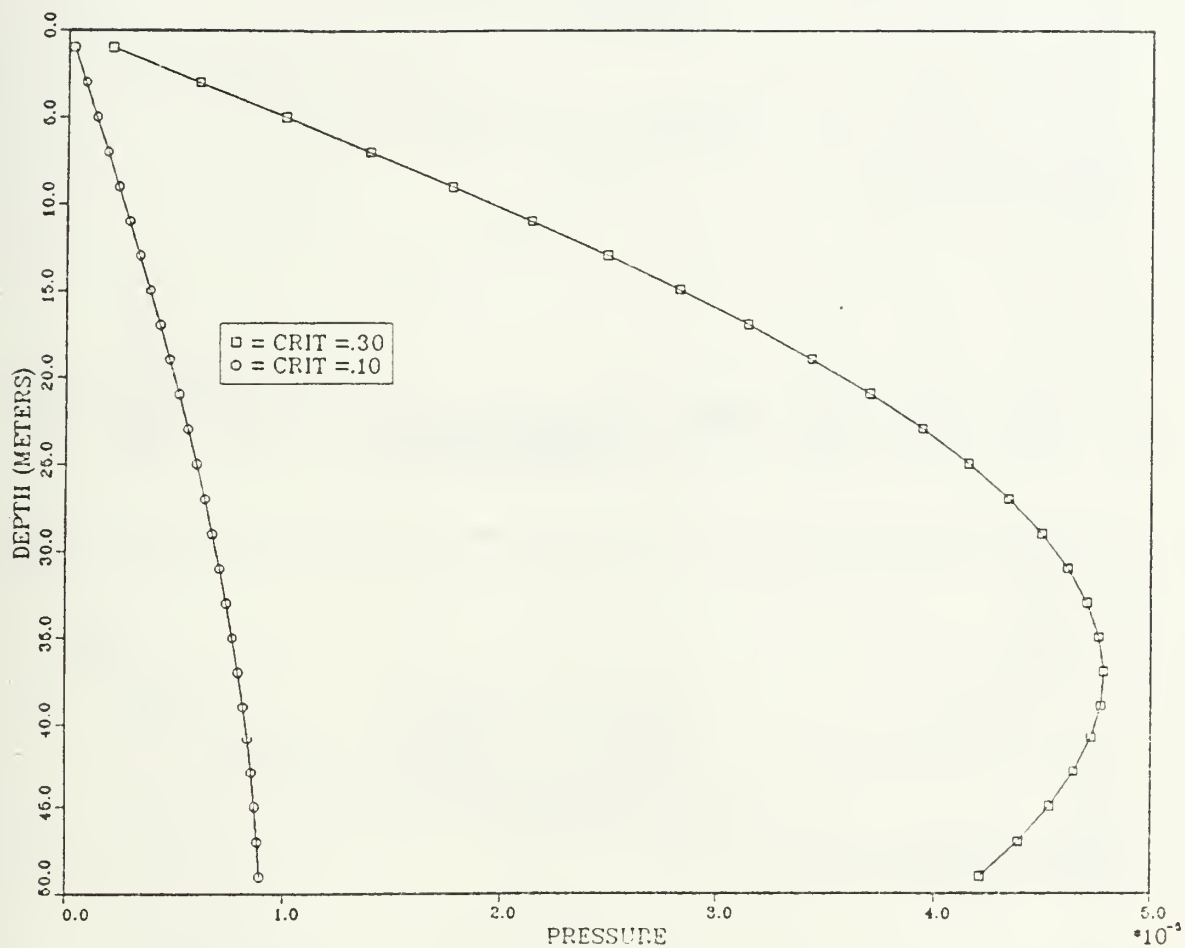


Figure 4.15. Loss Bounce (Upper) and Loss/Meter (Lower)  
Due to Bottom Interaction.





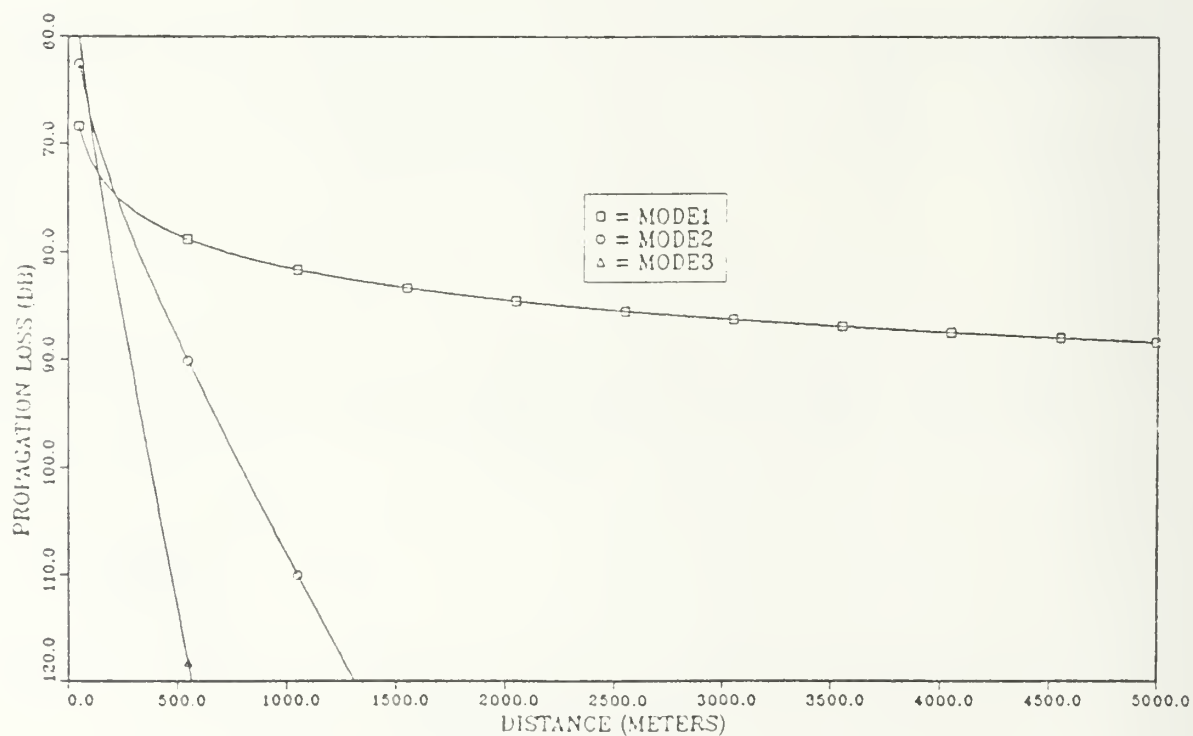


Figure 4.17. Propagation Loss for Each Mode When Critical Angle is Less Than Grazing Angle for All Modes (Upper) and For Mode 1 Only (Lower).

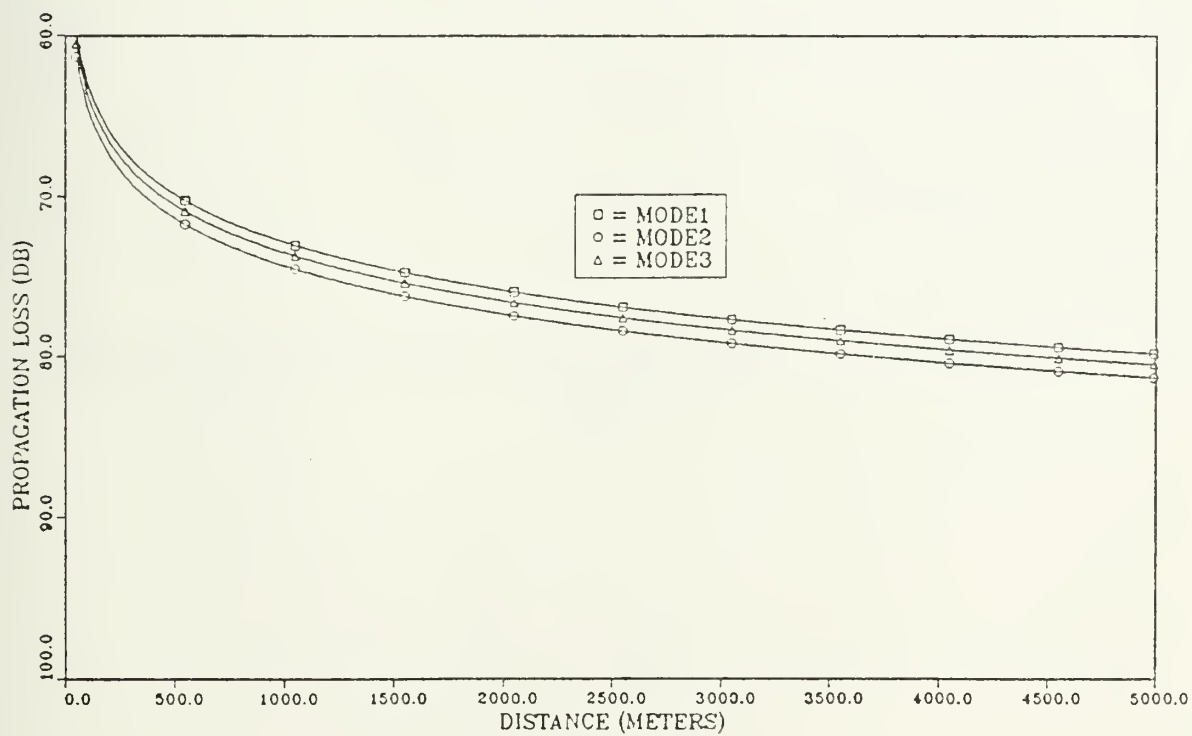
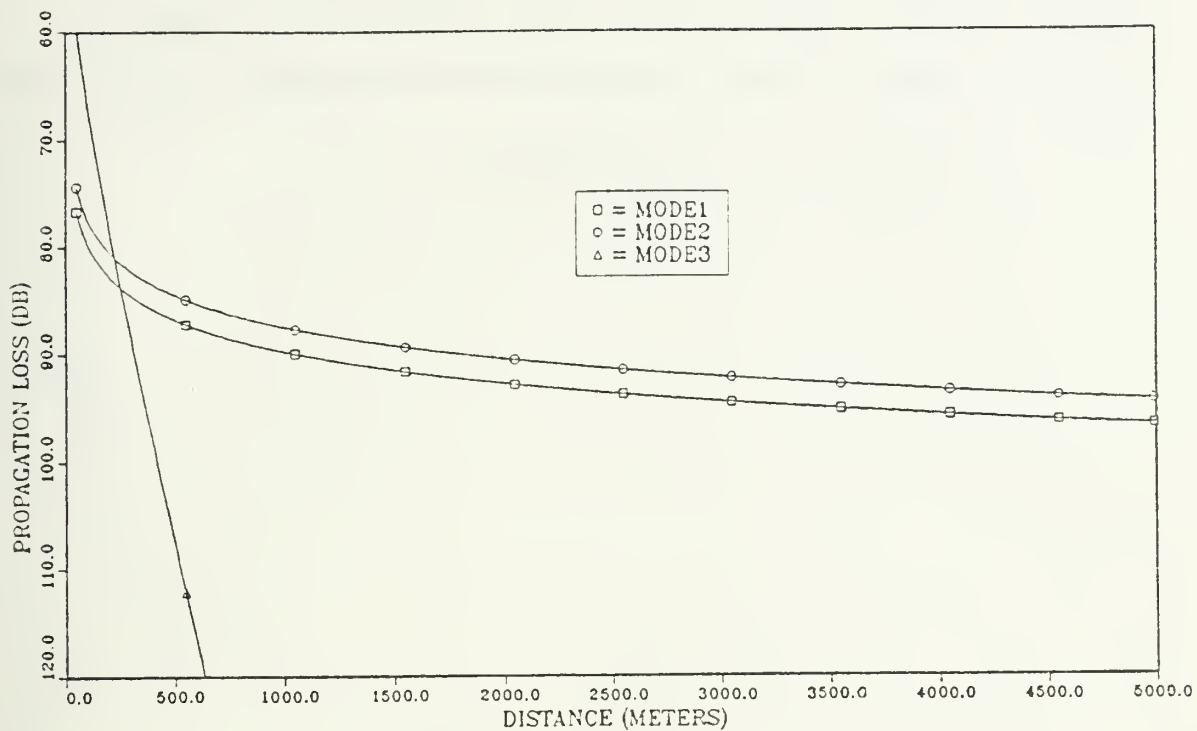


Figure 4.18. Propagation Loss for Each Mode When Critical Angle Less Than Grazing Angle for Modes 1 and 2 Only (Upper) and for Modes 1, 2, and 3 (Lower).

positive gradient case when the critical angle was 0.1 radians. It can be seen in Figure 4.19 that the upward refraction caused by the gradient lessens loss due to bottom interactions.

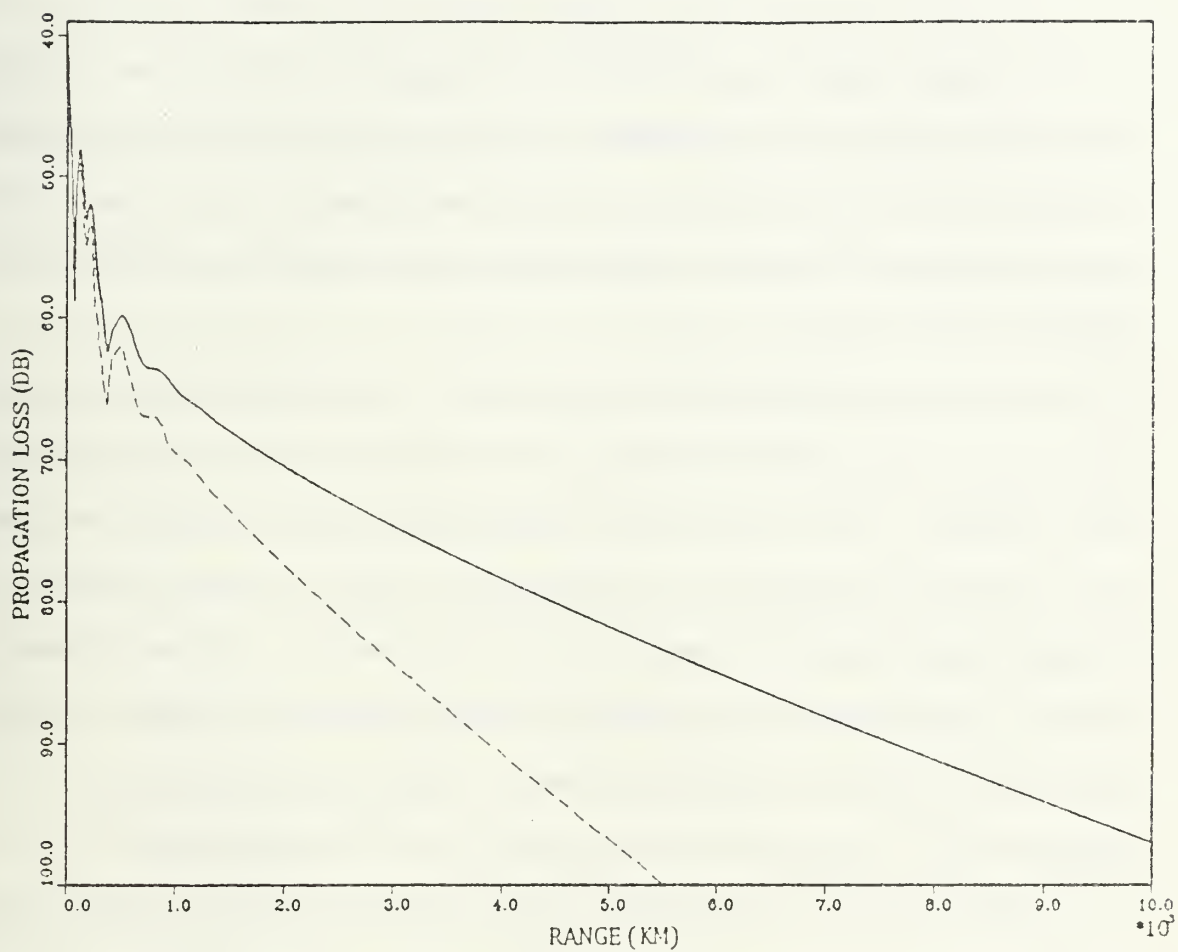


Figure 4.19. Propagation Loss with Impedance Bottom for Isovelocity Water Conditions (Dashed Lines) and Strong Positive Gradient (Solid Line).

## V. CONCLUSION

The program EXACT, which computes propagation loss by first solving for individual mode wave numbers, was found to give realistic values. The Fast Field Program, which was meant to solve for loss using an FFT was not completed because of complications that proved unsolvable in the limited time available.

One of the problems with the solution of the program EXACT, which would also be a problem with FFP, is the restriction placed on the impedance bottom. All of the sound transmitted into the bottom is considered lost to the bottom. No allowance is made for this energy to be refracted upward and re-transmitted into the water. This might not be entirely unrealistic in some cases, because bottom absorption is often very high. However, this simplification limits the practicality of this program and is considered by the author to be its main weakness.

Another point of consideration is the number of modes involved. The tests run usually involved only three real modes, two of which are lost to the bottom after a short range when the critical angle is 0.1 radians (sound speed ratio is 1.005:1). An increase of depth or frequency will mean an increased number of modes. There might be 4, 400, or 40,000 modes present but a large portion of them may suffer a large bottom loss. This also explains why trapped modes are so significant and why it is often sufficient to consider only a few modes in most analyses.

One of the intended purposes of the thesis was to compare the computer processing time for each program to solve for conditions where a large number of modes were present. It was reasoned that an increase of frequency and/or depth would require a proportionate increase in the number of depth samples used by the subroutines that calculated pressure as a function of depth for each horizontal wave number. This would mean that if the frequency were increased from 50 to 100 Hertz and the depth from 50 to 500 meters, there would be a 20 fold increase in the processor time used to do these calculations in each of EXACT and FFP. However, there would be a further 20 fold increase in time for EXACT because it would be required to calculate for 20 times as many modes. The FFP would not require any similar increase and would therefore have a decided advantage when a large number of modes were involved. It is possible that for cases with a small number of modes, EXACT would be faster, but the information was not available for comparison.

A simplification in EXACT involves the accuracy criterion of the horizontal wave number. It was decided that errors due to accuracy limitations would be acceptable if the wave number were resolved to less than  $10^{-6}$ . However, the subroutines 'eigens', 'modes1', and 'modes2' return the square of the wave number. For the calculated  $\xi_n$  to remain within the limit,

$$\xi_n^2 + |\text{Error}| < (\xi_n + 10^{-6})^2$$

so

$$|\text{Error}| < 2 \times 10^{-6} \xi_n.$$

For the conditions considered, the correct accuracy criteria should have been marginally more restrictive for all three modes considered. Had any very small wave numbers resulted, the allowable accuracy criteria should have been much more restrictive. A more complete program would calculate each wave number to its own allowable accuracy limit using formula 5.1

While it is recognized that program results would in no way alter the facts of nature, the correspondence between observed phenomena and predicted results did add to the credibility of the theory and program outlined in this thesis. Many of the results, as illustrated in the graphs, would prove useful as teaching aids to elucidate the principles of sound propagation in the ocean. Without reference to the development of normal mode theory, it is possible to illustrate the consequences of changing depth, range, frequency, water depth, and sound speed profiles. For example, the program could be used to show the effects of surface duct on long range propagation.

Finally, it is realized that the programming methods used are far less efficient than many readily available programs. The intention of this thesis was to develop an individual Normal Mode program from a theoretical basis without direct reference to other, more sophisticated programs. A more complete study would compare program results to actual observed data as well as to results of other, more authoritative predictions.



## APPENDIX A

### MATRIX METHOD FOR FINDING MODAL HORIZONTAL WAVE NUMBERS

The matrix method (Ref.8) employed in the program EXACT yields a complete set of eigenvalues in a single pass utilizing IMSL routine EQRTIS. It is convenient, fast and has the advantage that all modes are assuredly determined, no matter how close together they are. Accuracy is not attempted; that is assured with the Runge-Kutta routines that are used subsequently.

The Matrix solution is a means of solving for the eigenvalues of the one dimensional differential equation:

$$\frac{d^2\phi}{dz^2} + k_z^2\phi = 0 \quad \text{A.1}$$

where:

$\phi$  is the eigenfunction,

$k_z$  is the vertical wave number  $\sqrt{(k^2 - \xi^2)}$ ,

$\xi$  is the horizontal wave number, and

$z$  is the depth.

It solves the equation by finding the eigenvalues of the matrix M in the following Matrix equation:

$$M\psi = -(\Delta z)^2 E\psi \quad \text{A.2}$$

This equation results from writing the differential equation as a finite-difference equation at each of N depth  $\Delta z$  apart.  $\psi$  a column matrix with N elements, each element defined by:

$$\psi_n = \psi(n\Delta z) \quad n = 1, 2, \dots, N \quad A.3$$

and M is a square symmetric tridiagonal matrix which allows a computationally efficient means of finding the eigenvalues.

$$M = \begin{pmatrix} D_1 & -1 & 0 & - & - & - & - & 0 \\ -1 & D_2 & -1 & - & - & - & - & 0 \\ 0 & -1 & D_3 & -1 & - & - & & \\ & - & - & - & - & - & - & - \\ & - & - & - & - & - & - & - \\ 0 & - & - & - & - & -1 & D_{N-1} & -1 \\ 0 & - & - & - & - & 0 & -1 & D_N \end{pmatrix} \quad A.4$$

where:

$$D_n = 2 - (\Delta z)^2 k^2(n\Delta z) \quad n = 1, 2, \dots, N \quad A.5$$

# APPENDIX B

## COMPUTER PROGRAM EXACT

FILE: EXACT FORTRAN 3.1

```

C*  MAIN PROGRAM READS UP TO 30 PAIRS OF SOUND VELOCITY INFORMATION
C*  IT ASSIGNS CALCULATED VALUES OF WAVENUMBER FOR EACH INCREMENTAL
C*  DEPTH AND CALCULATES THE NUMBER OF REAL EIGENVALUES AS WELL AS
C*  MAX WAVENUMBER AND THE DEPTH INCREMENT
C*  ABSORPTION IS ASSUMED TO BE CONSTANT AT ALL DEPTHS
C*  NON-COMPLEX EIGENVALUES ARE CALCULATED BY A MATRIX METHOD IN
C*  SUBROUTINE EIGENS AND THESE ARE USED AS A FIRST ESTIMATE IN ONE
C*  OF MODES SUBROUTINES
C*  PRESSURES AND THE WRONSKIAN FROM MODES ARE USED TO CALCULATE
C*  COMPLEX INDIVIDUAL MODAL PRESSURES WHICH ARE SUMMED FOR
C*  PARTICULAR RANGES
C*  BOTTOM ABSORPTION NOT ACCOUNTED FOR
C*
C*****
      COMPLEX K(10001),P(10001),CALC(50),ARGUE,VAL,CORR,INT,PDIFF,PTM,
      1PRX,DENOM,PPRESS(50),EIG(50),PRESS(50),PRESSR,IMAG,ALFA,AIG(50),
      1EFACT,REF,COMP
      REAL D(30),KAY(30),RATE(30),C(30),EIG2(50),MAG(50),KMAX,K1,
      1KAE(10001),KAA(10001),PR(50),PII(50)
      LOGICAL TOP
C
      TOP = .FALSE.
      NUM=1
      PI = 3.141592654
      CMAX=0
      CMIN=200
C
      FREQ = 50
      DEPTH = 10
      DEPTH = 37
      RMIN = 20
      INC = 400
      JUMP = INC/100
      ERRMAX = .00000001
      CORN = 2
      CRITA = .15
      RATIO = 2.0
12  READ (3,*) D(NUM),C(NUM)
C
C*****
C*  EACH SOUND VELOCITY/DEPTH PAIR HAS A WAVENUMBER CALCULATED
C*****
C
      IF (D(NUM) .LT. 0) GOTO 14
      KAY(NUM) = 2 * PI * FREQ / C(NUM)
      IF (C(NUM).GT.CMAX) THEN
        CMAX=C(NUM)
      END IF
      IF (C(NUM).LT.CMIN) THEN
        KMAX=KAY(NUM)
        CMIN = C(NUM)
      END IF
      IF (NUM .EQ. 1) GOTO 13
C
      RATE (NUM-1) = (KAY(NUM) - KAY(NUM-1)) / (D(NUM)-D(NUM-1))

```

FILE: EXACT      FORTRAN A1

```

      PRINT 103,D(NUM-1),C(NUM-1),KAY(NUM-1),RATE(NUM-1)
C
13   NUM = NUM + 1
      GOTO 12
14   BOTTOM=D(NUM-1)
      N = IFIX((4*BOTTOM*FREQ/CMAX + 1)/2.0)
      WRITE(4,6389) N
6389 FORMAT (// ' THERE ARE ',I6,' REAL MODES'//)
      M = 1 + N
      DELZ = BOTTOM/(INC*N)
      PRINT 103,D(NUM-1),C(NUM-1)
      WRITE (4,103)D(NUM-1),C(NUM-1),KAY(NUM-1)
      IF (C(NUM-1).LT.C(1)) TOP = .TRUE.
      IF (N.GT.50) THEN
100      FORMAT('TOO MANY MODES FOR THIS PROGRAM!!    N(REAL) = ',I4)
          GOTO 11
      END IF
C
C*****
C*
C*    THE NEXT SECTION CALCULATES THE EXACT WAVENUMBERS FOR THE SUB-
C*    ROUTINES EIGENS, MODES1 AND MODES2
C*    THE REAL COMPONENTS FOR MODES1 AND MODES2 ARE CALCULATED FOR
C*    INC*N + 1 DEPTHS STARTING WITH DEPTH 1 AT THE SURFACE AND INC*N+1
C*    AT THE BOTTOM
C*    AT REGULAR DEPTH INCREMENTS A REAL VALUE OF K IS TAKEN FOR
C*    USE IN SUBROUTINE EIGENS            THE NUMBER OF SAMPLES IS 100
C*
C*****
C
      KOUNT = 0
      NUM = 1
      DO 18 IG = 1, INC*N+1
          DP = (IG-1) * DELZ
          KAA(IG) = KAY(NUM) + RATE(NUM)*(DP-D(NUM))
C*****
C    IT IS POSSIBLE TO INSERT A LOOP TO CHOOSE ONLY A FRACTION OF
C    THE DEPTH SAMPLES OF K( )    A TEST RUN WAS MADE TO COMPARE THE
C    VALUES OBTAINED FOR VARIOUS 'JUMPS'
C*****
          IF (INC.LE.200) JUMP = 2
          IF (MOD (IG-1,JUMP) .EQ. 0) THEN
              KOUNT = KOUNT + 1
              IF (IG.EQ.1) THEN
                  KOUNT = 0
                  GOTO 886
              ENDIF
              KAE(KOUNT) = KAA(IG)
886      END IF
          IF (DP.GE.D(NUM + 1)) NUM = NUM + 1
18   CONTINUE
C
      CALL EIGENS(BOTTOM,KOUNT,M,KAE,EIG2,RMIN)
C

```

FILE: EXACT      ECHOIR N A1

```

C*****
C*      ABSORPTION IN NEPERS/METER CALCULATED AS FUNCTION OF FREQ
C*****
      FREK = FREQ/1000
      FREEK = FREK**2
      ALFAW = .00001*FREEK/(1+FREEK)
C
C*****
C*      NEXT FOLLOWS A LOOP WHICH CAN BE USED TO DETERMINE THE PRESSURE
C*      OR ATTENUATION AT ALL DEPTHS FROM TOP TO BOTTOM
C*****
C
      DO 54 IDR = 37,37
      DEPTH = 1.0*IDR
      DO 55 I =1,M
        CRIT=CRITA
        NC = 1
        ALFAB = 0.0
        ALFAT = ALFAW + ALFAB
        ALFA = CMPLX(0.0,ALFAT)
5500      DO 598 IK = 1,INC*N+1
          K(IK) = KAA(IK) + ALFA
598      CONTINUE
          ARGUE=K(20)**2-(PI*(I-.5)/BOTTOM)**2
          CALC(I) = CSQRT(ARGUE)
C*****
C*      CALC IS USED TO EVALUATE THE CORRECTNESS OF THE PROGRAM
C*      BY INPUTTING AN ISOVELOCITY PROFILE IT IS POSSIBLE TO CALCULATE
C*      THE CORRECT HORIZONTAL WAVENUMBER FOR EACH MODE AND THEN COMPARE
C*      THE RESULTS OF THE PROGRAM TO THIS 'CORRECT' ANSWER
C*****
          VAL = EIG2(I)
          CORR = 1
C
          IF (TOP) THEN
C*****
C*      IF THE SOUND VELOCITY IS GREATER AT THE TOP THAN AT THE BOTTOM
C*      THEN SUBROUTINE MODES1 IS USED; OTHERWISE MODES2 IS USED
C*      AFTER EACH RUN OF EITHER SUBROUTINE, THE CORRECTION MADE TO THE
C*      SQUARE OF THE HORIZONTAL WAVELENGTH IS COMPARED TO A ERROR
C*      CRITERION; IF IT EXCEEDS THE SET LIMIT THE SUBROUTINE IS CALLED
C*      AGAIN. IF THE CORRECTION IS LESS THAN THE LIMIT, THE PROGRAM
C*      PROGRESSES AND SOLVES FOR THE PRESSURE FOR THAT MODE
C*****
C*
180      CALL MODES1(VAL,DELZ,N,K,P,CORR,INT,INC,RATIO,CRIT,CORRN,I)
          NC = NC + 1
C          IF(CABS(VAL).GT.CABS(K(INC*N+1)**2))THEN
C              CRIT =.5*CRIT
C              CORRN = CORN
C              IF (CRIT.LT..005) GO TO 66
C              VAL = EIG2(I)
C              GOTO 180
C          ENDF
          IF(CABS(CORR).GT.ERRMAX) GOTO 180

```

FILE: EXACT FORTKAN A1

```

C          IF (CRIT.LT.CRITA) THEN
C              CRIT = CRITA
C              GOTO 180
C          ENDIF
C          GOTO 57
C56        WRITE(4,570)I
C
C          IF (VAL.EQ.0) THEN
C          ELSE
190          CALL MODES2(VAL,DELZ,N,K,P,CORR,INT,INC,RATIO,CRIT,CORRN,I)
              NC = NC + 1
              IF(CABS(VAL).GT.CABS(K(INC*N+1)**2))THEN
                  CRIT = .5*CRIT
                  CORRN = CORN
                  IF (CRIT.LT..005) GO TO 56
                  VAL = EIG2(I)
                  GOTO 190
              ENDIF
              IF(CABS(CORR).GT.ERRMAX) GOTO 190
              IF (CRIT.LT.CRITA) THEN
                  CRIT = CRITA
                  GOTO 190
              ENDIF
              GOTO 57
56          WRITE(4,570)I
570         FORMAT(' NO CONVERGENCE!!!! FIND THE ERROR'.I6)
57         END IF
          EIG(I) = CSQRT(VAL)
          IDT1 = IFIX(DEPTHT/(DELZ**2))*2
          IDT2 = IDT1 + 2
          PDIFF = P(IDT2) - P(IDT1)
          DDIFF = DEPTHT - (IDT1)*DELZ
          PTX = P(IDT1) + PDIFF*DDIFF/(DELZ**2)
          IDR1 = IFIX(DEPTHR/(DELZ**2))*2
          IDR2 = IDR1 + 2
          PDIFF = P(IDR2) - P(IDR1)
          DDIFF = DEPTHR - (IDR1)*DELZ
          PRX = P(IDR1) + PDIFF*DDIFF/(DELZ**2)
          AIG(I) = CMPLX(REAL(EIG(I)),ABS(AIMAG(EIG(I))))
          DENOM = INT*CSQRT(AIG(I)*PI/2)
          PPRESS(I)=PTX*PRX/DENOM
C*****
C    FOLLOWING INSTRUCTIONS ONLY FOR CALC OF RAYLEIGH COEFFICIENTS
C    DONE FOR RANGE OF CRITICAL ANGLES AND FOR DIFFERENT IMPEDANCE RATIOS
C*****
55    CONTINUE
C
C
C*****
C*    THE FOLLOWING LOOP CALCULATES THE ATTENUATION OF THE SIGNAL AT
C*    DIFFERENT RANGES BY SUMMING THE COMPLEX PRESSURE DUE TO THE
C*    INDIVIDUAL MODES
C*    CAN BE SET UP TO PRODUCE ATTENUATION AT REGULAR RANGE INTERVALS
C*    OR AT IRREGULAR INTERVALS SUCH AS EVERY 10 METERS OUT TO 100
C*    METERS, THEN EVERY 100 METERS TO 1000 AND SO ON.

```

FILE: ENACT      FORTTRAN A1

```

C*
C*****
      IMAG=CMPLX(0,1)
      DO 560 IRNG =1,1

          DO 561 NRNG = 300,3000
              R=(10**IRNG)*NRNG
          C      R = 50000
              PRESSR = 0
              STRONG = 0
              DO 562 I = 1,N
                  PRESS(I)=PPRESS(I)*CEXP(IMAG*EIG(I)*R)/SQRT(R)
                  MAG(I)= CABS(PRESS(I))
                  PRESSR= PRESSR + PRESS(I)
                  PR(I)=REAL(PRESSR)
                  PIM(I) = AIMAG(PRESSR)
                  FASE = ATAN(AIMAG(PRESSR)/REAL(PRESSR))
                  STRONG=CABS(PRESSR)
          C      WRITE (4,3434)I, PRESS(I),PPRESS(I)
          C      3434      FORMAT(I6,4E15.7)
          C      PRINT 3487,MAG(I),STRONG
          C      3487      FORMAT(2F15.5)
              FACT = CSQRT(K(INC*N+1)**2 - (EIG(I)/COS(CRITA))**2)
              REF = (RATIO - FACT)/(RATIO + FACT)
              FRACT = CABS(REF)
              COMP = CSQRT(K(INC*N+1)**2-EIG(I)**2)/(2*K(INC*N+1)*BOTTOM)
              QLOS = (1-FRACT)*CABS(COMP)
              PHAS = ATAN(AIMAG(REF)/REAL(REF))
              THETA = ARCOS(EIG(I)/K(INC*N+1))
          C
          C      562      CONTINUE
          C      510      CONTINUE
              ATTEN = -20*ALOG10(STRONG)

          C      561      CONTINUE
          C      560      CONTINUE

          C      54      CONTINUE
          C      11      STOP
          C      END

      SUBROUTINE MODES1(VAL,DELZ,N,K,P,CORR,INT,INC,RATIO,CRIT,CORRN,I)
      COMPLEX K(10001),P(10001),VAL,CORR,INT,F1,A1,B1,F2,A2,B2,F3,A3,
      1B3,F4,B,A,IMAG,AP,DENO
  C
  C*****
  C*      THIS SUBROUTINE USES A FOURTH ORDER RUNGE KUTTA TECHNIQUE
  C*      TO CALCULATE PRESSURE AND ITS DERIVATIVE STARTING AT THE SURFACE
  C*      AND STEPPING DOWN A DISTANCE 2 TIMES THE DEPTH INCREMENT UNTIL
  C*      THE BOTTOM IS REACHED
  C*      CALC AT EACH L IS IN FACT FOR THE L+1 STEP
  C*      AT THE BOTTOM THE CALCULATED PRESSURE, DERIVATIVE AND INTEGRAL
  C*      ARE USED TO DETERMINE THE CORRECTION TO BE APPLIED TO THE
  C*      SQUARE OF THE BEST GUESS OF THE NORMAL MODE HORIZONTAL WAVE-

```



FILE: EXACT      FORTRAN A1

```

C*      NUMBER      THE CORRECTION IS APPLIED AND THE RESULT IS PASSED BACK
C*      TO THE MAIN PROGRAM
C*      IN ADDITION THE PRESSURE AT ALL DEPTH INTERVALS IS PASSED BACK
C*      THIS IS USED IN THE CALCULATION OF ATTENUATION
C*      SHOULD SAVE ONLY THOSE PRESSURES REQUIRED NOT; ALL INC*N+1
C*****
      PI = 3.141592654
      INT = 0.0
      B = 0.0
      P(1) = B
      A = 1.
      DO 18 L = 1, INC*N - 1, 2
C
      DP = DELZ*(L+1)
      F1 = -B * (K(L))**2 - VAL)
      A1 = A + DELZ*F1
      B1 = B + DELZ*A
C
      F2 = -B1*(K(L+1))**2 - VAL)
      A2 = A + DELZ * F2
      B2 = B + DELZ *A1
C
      F3 = -B2*(K(L+1))**2 - VAL)
      A3 = A + 2*DELZ*F3
      B3 = B + 2*DELZ*A2
C
      F4 = -B3*(K(L+2))**2 - VAL)
      B = B + 2*DELZ*(A + 2*A1 + 2*A2 + A3)/6
      P(L+1) = B
      A = A + 2*DELZ*(F1 + 2*F2 + 2*F3 + F4)/6
      INT = INT + B**2*DELZ*2
C
18  CONTINUE
      IMAG = CMPLX(0.0, 1.0)
      FILL = REAL(K( INC*N+1 ))**2
      DENO = CSQRT((FILL - VAL)/FILL)
      AP = CSQRT(FILL-VAL/COS(CRIT)**2)*B*IMAG/RATIO*DENO
      CORR = B*(A+AP)/INT
      VAL = VAL - CORR/CORRN
21  RETURN
      END

      SUBROUTINE MODES2 (VAL,DELZ,N,K,P,CORR,INT,INC,RATIO,CRIT,CORRN,1,
      COMPLEX K(10001),P(10001),VAL,CORR,INT,F1,A1,B1,F2,A2,B2,
      F3,A3,B3,F4,B,A,IMAG,DENO
C
C*****
C*      THIS SUBROUTINE USES A FOURTH ORDER RUNGE KUTTA TECHNIQUE
C*      TO CALCULATE PRESSURE AND ITS DERIVATIVE STARTING AT THE BOTTOM
C*      AND STEPPING UP A DISTANCE OF 2 TIMES THE DEPTH INCREMENT UNTIL
C*      THE SURFACE IS REACHED
C*      CALC AT EACH L IS IN FACT FOR THE L-1 STEP
C*      AT THE TOP, THE CALCULATED PRESSURE, DERIVATIVE AND INTEGRAL
C*      ARE USED TO DETERMINE THE CORRECTION TO BE APPLIED TO THE

```

FILE. EXACT 1001.00 A1

```

C*   SQUARE OF THE BEST GUESS OF THE NORMAL MODE HORIZONTAL WAVE-
C*   NUMBER   THE CORRECTION IS APPLIED AND THE RESULT IS PASSED BACK
C*   TO THE MAIN PROGRAM
C*   IN ADDITION THE PRESSURE AT ALL DEPTH INTERVALS IS PASSED BACK
C*   THIS IS USED IN THE CALCULATION OF ATTENUATION
C*****
  PI = 3.141592654
  INT = 0
  LFLOOR = INC*N + 1
  B = 1.
  P(INC*N) = B
  IMAG = CMPLX(0.0,1.0)
  FILL = REAL(K(LFLOOR))**2
  DENO = CSQRT((FILL - VAL)/FILL)
  A = CSQRT(FILL-VAL/COS(CRIT)**2)*B*IMAG/RATIO/DENO
  A = 0.
  IF (I.GT.N) A = 0.
  DO 28 L = 1, INC*N-1, 2
C
    DP = DELZ*(LFLOOR-L-2)
    F1 = -B * (K(LFLOOR-L+1)**2 - VAL)
    A1 = A + DELZ*F1
    B1 = B + DELZ*A
C
    F2 = -B1*(K(LFLOOR-L)**2 - VAL)
    A2 = A + DELZ*F2
    B2 = B + DELZ*A1
C
    F3 = -B2*(K(LFLOOR-L)**2 - VAL)
    A3 = A + 2*DELZ*F3
    B3 = B + 2*DELZ*A2
C
    F4 = -B3*(K(LFLOOR-L-1)**2 - VAL)
    B = B + 2*DELZ*(A + 2*A1 + 2*A2 + A3)/6
    P(LFLOOR-L-2) = B
    A = A + 2*DELZ*(F1 + 2*F2 + 2*F3 + F4)/6
    INT = INT + B**2*DELZ*2
C
28  CONTINUE
    CORR = B*A/INT
    VAL = VAL + CORR/CORRN
21  RETURN
    END

SUBROUTINE EIGENS(BOTTOM,KOUNT,M,KAE,EIG2,RMIN)
  DIMENSION E(10001),D(10001),AK2(10001),EIG2(50),EIG(50)
  REAL KAE(10001)
  PRINT 4856,BOTTOM,KOUNT,M,RMIN
C*****
C*
C*   COMPLEX NOT USED IN THIS SUBROUTINE BECAUSE IT CALLS IMSL
C*   SUB EQRT1S AND IT IS IMPRACTICAL TO MODIFY THAT FOR COMPLEX
C*   THE REAL EIGENVALUES ARE THEREFORE CALCULATED AND USED IN
C*   MODES1 AND MODES2 WHERE COMPLEX EIGENVALUES ARE USED

```

FILE= EXACT FORTRAN A1

```

C*
C*
C*   THIS SUBROUTINE IS NOT USED IN THE FFT PROGRAM
C*
C* *****
      DZ = BOTTOM/(KOUNT-1)
      DZ2 = DZ*DZ
C
      DO 100 I=1,KOUNT
        AK2(I) = KAE(I)**2
        D(I) = -AK2(I)*DZ2 + 2.0
        E(I) = 1.0
      100 CONTINUE
C
      D(KOUNT) = D(KOUNT) - 1.0
      E(1) = 0.0
      ISW = 0
      IER = 0
      CALL EQRT1S (D,E,KOUNT,M,ISW,IER)
C
      DO 6000 J = 1,M
        EIG2(J) = -D(J)/DZ2
C*****
C   ALTHOUGH THE FORMULA IS EXACT THE SUBROUTINE RUNS IN SINGLE
C   PRECISION SO ONE MUST BE CAREFUL
C*****
        EIG2EX = AK2(20) - (3.1415926535*(2*J-1)/(2.0*BOTTOM))**2
      6000 CONTINUE
C
      9000 FORMAT (15,3F16.10)
      8000 RETURN
      END

```

# APPENDIX C

## COMPUTER PROGRAM FFP

```

FILE: FFP      FORTRAN A1

      COMPLEX WRON,U,DU,V,DV,V1,DV1,K(25000),EN,EIGVAL,VAL,IMAG,FUNC,
1AREA,SIMPLE,SOLN,VEE,YEW,VRTWN,WRONK
      REAL KMAX,D(30),KAY(30),RATE(30),C(30)
C
      NUM=1
      PI = 3.14159265
      CMAX=0
      CMIN=2000
C
      FREQ = 50
      DEPTH = 10
      DEPTH = 37
      RMIN = 40
C*****
C      INC , THE NUMBER OF INCREMENTS PER REAL MODE, MUST BE EVEN)
C*****
      INC = 200
12  READ (3,*) D(NUM),C(NUM)
C
      IF (D(NUM) .LT. 0) GOTO 14
      KAY(NUM) = 2 * PI * FREQ / C(NUM)
      IF (C(NUM).GT.CMAX) THEN
          CMAX=C(NUM)
          DMAX=D(NUM)
      END IF
      IF (C(NUM).LT.CMIN) THEN
          KMAX=KAY(NUM)
          DKMAX=D(NUM)
          CMIN = C(NUM)
      END IF
      IF (NUM .EQ. 1) GOTO 13
C
      RATE (NUM-1) = (KAY(NUM) - KAY(NUM-1)) / (D(NUM)-D(NUM-1))
C
13  NUM = NUM + 1
      GOTO 12
14  BOTTOM=D(NUM-1)
      N = IFIX(2*BOTTOM*FREQ/CMAX+.5)
      INCTOT = INC*N
      IF (INCTOT.GT.18000) INCTOT = 18000
      DELZ = BOTTOM/INCTOT
      IF (N.GT.50) THEN
          WRITE(4,100) N
100  FORMAT('TOO MANY MODES FOR THIS PROGRAM!!  N(REAL) = ',I4)
          GOTO 11
      END IF
C
C*****
C      VALUE OF ABSORPTION DEPENDENT ON FREQUENCY ONLY-NO TEMP DEPENDENCE)
C
C*****
      FFREQ = FREQ/1000
      ALFA1 = .0000092/(.7 + FFREQ**2)
      ALFA2 = .0046/(6000 + FFREQ**2)

```

FILE: TFP            FORTRAN A1

```

      ALFA3 = .0000000046
      ALFA = (ALFA1 + ALFA2 + ALFA3) * FFREQ**2
      ALFA = .00001
C      ALFA = 0
C**** EXAGGERATE ALFA TO SEE IF NUMBER OF ITERATIONS IMPORTANT
      NUM = 1
      DO 18 IG = 1, INC*N + 1
        DP = (IG-1) * DELZ
        K(IG) = KAY(NUM) + RATE(NUM)*(DP-D(NUM))
        IF (DP.GE.D(NUM + 1)) NUM = NUM + 1
18     CONTINUE
C
      IF (DEPTHT.GT.DEPTHR) THEN
        DUP = DEPTHR
        DLW = DEPTHT
      ELSE
        DLW = DEPTHR
        DUP = DEPTHT
      ENDIF
C
      IU1 = IFIX(DUP/(DELZ*2))*2
      IU2 = IU1 + 2
      IL1 = IFIX(DLW/(DELZ*2))*2
      IL2 = IL1 + 2
C
C
C*****
C      ALFA IS CALCULATED FOR ONE FREQUENCY AND IS PART OF VAL(COMPLEX)
C
C*****
C
      AREA = 0.0
      IFFP = 2047
      DO 55 I =1, IFFP
C
C*****
C
C      DURING THIS PHASE OF THE PROGRAM MODES2 PROVIDES VALUES FOR
C      PRESSURE AND DERIVATIVE AT BOTH THE TRANSMITTER AND THE RECEIVER
C      STARTING WITH THE INITIAL CONDITIONS AT THE SURFACE
C      (IE PRESSURE = 0 AND DERIV IS AN ARBITRARY VALUE)
C      MODES 2 PROVIDES VALUES FOR PRESSURE AND DERIVATIVE FOR THE
C      LOWER POINT ONLY STARTING WITH THE INITIAL CONDITIONS AT THE
C      BOTTOM (IE DERIVATIVE = 0 AND PRESSURE IS AN ARBITRARY VALUE
C      A VALUE FN REPRESENTS THE CONTRIBUTION OF EACH 'INCREMENT'
C      AND THE AREA UNDER THE FN CURVE REPRESENTS THE TOTAL 'PRESSURE
C
C*****
C
      R = 500
      WVMNCH = 1.1*KMAX/IFFP
      WVMN = I*WVMNCH
      EIGVAL = CMPLX(WVMN,ALFA)
      VAL = EIGVAL**2
      CALL MODES1(VAL,DELZ,INCTOT,K,U,DU,IU1,IU2,DUP,DLW,V1,DV1,

```

FILE: FEP      FORTRAN A1

```

1  IL1,IL2)
   CALL MODES2(VAL,DELZ,INCTOT,K,V,DV,IL1,IL2,DLW,INC)
   WRON = V*DV1-V1*DV
878  FORMAT (10E3.1)
C*****
C  CALCULATE PARTIAL FIELD INTEGRAL FOR PARTICULAR VALUE OF
C  WAVENUMBER COMPARE TO THAT CALCD BY PROGRAM
C*****
C  VRTWN = CSQRT(K(20)**2 - VAL)
C  YEW = SIN(VRTWN*DUP)
C  VEE = COS(VRTWN*(BOTTOM-DLW))
C  WRONK = VRTWN*COS(VRTWN*BOTTOM)
C  SOLN = YEW * VEE / WRONK
C  SIMPLE = U*V/WRON
C  FN = U*V*CSQRT(EIGVAL)/WRON
C  IMAG = CMPLX(0,1)
C  FUNC = FN*CEXP(IMAG*EIGVAL*R)*SQRT(2/(PI*R))
C  CONT = CABS(FUNC)
C  AREA = AREA + FUNC*WVNMCH
C  TOTAL = CABS(AREA)
C  IF (MOD(I,5).EQ.0) WRITE (4,190) EIGVAL,CONT,TOTAL
C  IF(MOD(I,100).EQ.0) PRINT 190, EIGVAL,CONT,TOTAL
55  CONTINUE
C
11  STOP
   END

C *****
C  MODES1 PROVIDES PRESS AND DERIV AT BOTH UPPER AND LOWER
C  INPUTS
C  VAL - THE INCREMENTAL HORIZONTAL WAVENUM - UP TO 8192 VALUES
C  DELZ- DEPTH INCREMENT FN OF DEPTH, NUMB OF MODES, AND NUMBER
C  OF INCREMENTS / MODE
C  N - NUMBER OF MODES
C  K - HORIZONTAL WAVENUMBER (COMPLEX) AT EACH DEPTH INCREMENT
C  DUP - DEPTH OF UPPER OF TXER AND RXER
C  DLW - DEPTH OF LOWER OF TXER RXER
C  IU1/IU2 INCREMENT NUMBER FOR INC ABOVE AND BELOW 'UPPER'
C  IL1/IL2 INCREMENT NUMBER FOR INC ABOVE AND BELOW 'LOWER'
C  INC - NUMBER OF INCREMENTS OF DEPTH
C  OUTPUTS
C  U1 - 'PRESSURE' AT UPPER
C  DU1 - 'DERIVATIVE AT UPPER
C  V1 - 'PRESSURE' AT LOWER
C  DV1 - 'DERIVATIVE' AT LOWER
C*****
C
C  SUBROUTINE MODES1(VAL,DELZ,INCTOT,K,U,DU,IU1,IU2,DUP,DLW,V1,DV1,
1  IL1,IL2)
C  COMPLEX K(25000),P(2),DP(2),DP1(2),P1(2),F1,A1,B1,F2,A2,B2,
1  F3,A3,B3,F4,A,B,PDIFF,P1DIFF,QDIFF,Q1DIFF,U,V1,DU,DV1,VAL
C
C  B = 0.0
C  A = .00001

```

FILE: SEP FORTRAN A1

```

DO 18 L = 1, INCTOT + 1, 2
C
    F1 = -B * (K(L)**2 - VAL)
    A1 = A + DELZ*F1
    B1 = B + DELZ*A
C
    F2 = -B1*(K(L+1)**2 - VAL)
    A2 = A + DELZ * F2
    B2 = B + DELZ *A1
C
    F3 = -B2*(K(L+1)**2 - VAL)
    A3 = A + 2*DELZ*F3
    B3 = B + 2*DELZ*A2
C
    F4 = -B3*(K(L+2)**2 - VAL)
    B = B + 2*DELZ*(A + 2*A1 + 2*A2 + A3)/6
    A = A + 2*DELZ*(F1 + 2*F2 + 2*F3 + F4)/6
C
    IF((L+1).EQ.IU1) THEN
        P(1) = B
        DP(1) = A
    ENDIF
    IF ((L+1).EQ.IU2) THEN
        P(2) = B
        DP(2) = A
    ENDIF
    IF ((L+1).EQ.IL1) THEN
        P1(1) = B
        DP1(1) = A
    ENDIF
    IF ((L+1).EQ.IL2) THEN
        P1(2) = B
        DP1(2) = A
    ENDIF
C
18  CONTINUE
    PDIFF = P(2) - P(1)
    P1DIFF = P1(2) - P1(1)
    QDIFF = DP(2) - DP(1)
    Q1DIFF = DP1(2) - DP1(1)
    DDIF1 = DUP - (IU1)*DELZ
    D1DIFF1 = DLW - (IL1)*DELZ
    U = P(1) + PDIFF*DDIF1/(DELZ*2)
    V1 = P1(1) + P1DIFF*D1DIFF1/(DELZ*2)
    DU = DP(1) + QDIFF*DDIF1/(DELZ*2)
    DV1 = DP1(1) + Q1DIFF*D1DIFF1/(DELZ*2)
21  RETURN
    END

C *****
C  MODES2 PROVIDES PRESS AND DER AT 'LOWER' ONLY
C  INPUTS
C    VAL - THE INCREMENTAL HORIZONTAL WAVENUM UP TO 8192 VALUES
C    DELZ- DEPTH INCREMENT FN OF DEPTH, NUMB OF MODES, AND NUMBER

```



FILE: FFF      FORTRAN A1

```

C      OF INCREMENTS / MODE
C      N - NUMBER OF MODES
C      K - HORIZONTAL WAVENUMBER (COMPLEX) AT EACH DEPTH INCREMENT
C      DUP - DEPTH OF UPPER OF TXER AND RXER
C      DLW - DEPTH OF LOWER OF TXER RXER
C      IU1/IU2 INCREMENT NUMBER FOR INC ABOVE AND BELOW 'UPPER'
C      IL1/IL2 INCREMENT NUMBER FOR INC ABOVE AND BELOW 'LOWER'
C      INC - NUMBER OF INCREMENTS OF DEPTH
C      OUTPUTS
C      U1 - 'PRESSURE' AT UPPER
C      DU1 - 'DERIVATIVE AT UPPER
C      V1 - 'PRESSURE' AT LOWER
C      DV1 - 'DERIVATIVE' AT LOWER
C
C*****
C
C      SUBROUTINE MODES2(VAL,DELZ,INCTOT,K,V,DV,IL1,IL2,DLW)
C      COMPLEX K(25000),P(2),DP(2),F1,A1,B1,F2,A2,B2,
C      IF3,A3,B3,F4,A,B,PDIFF,QDIFF,V,DV,VAL
C      B = .00001
C      A = 0.0
C      DO 28 L = 1, INCTOT+1,2
C
C          L1 = INCTOT - L - 1
C          F1 = -B * (K(L1)**2 - VAL)
C          A1 = A + DELZ*F1
C          B1 = B + DELZ*A
C
C          F2 = -B1*(K(L1-1)**2 - VAL)
C          A2 = A + DELZ*F2
C          B2 = B + DELZ*A1
C
C          F3 = -B2*(K(L1-1)**2 - VAL)
C          A3 = A + 2*DELZ*F3
C          B3 = B + 2*DELZ*A2
C
C          F4 = -B3*(K(L1-2)**2 - VAL)
C          B = B + 2*DELZ*(A + 2*A1 + 2*A2 + A3)/6
C          A = A + 2*DELZ*(F1 + 2*F2 + 2*F3 + F4)/6
C
C          IF((L1-2).EQ.IL1) THEN
C              P(1) = B
C              DP(1) = -A
C          ENDIF
C          IF((L1-2).EQ.IL2) THEN
C              P(2) = B
C              DP(2) = -A
C          ENDIF
C
C      28 CONTINUE
C          PDIFF = P(2) - P(1)
C          QDIFF = DP(2) - DP(1)
C          DDIFF = DLW - (IL1)*DELZ
C          V = P(1) + PDIFF*DDIFF/(DELZ*2)
C          DV = DP(1) + QDIFF*DDIFF/(DELZ*2)
C
C      21 RETURN
C      END

```

## LIST OF REFERENCES

1. Natural Bureau of Standards, AMS 55, Handbook of Mathematical Functions, by M. Abramowitz and I. Stegun, Washington 1972.
2. King, P., Use of Wavenumber Technique with the Lloyd's Mirror for an acoustic Doublet, Master's Thesis, Naval Postgraduate School, Monterey, California, June 1985.
3. Bucker, H.P., "Sound Propagation in a Channel with Lossy Boundaries," Journal of the Acoustical Society of America, V. 48 no. 5, November 1970.
4. Koch, R. A. and Lindberg, J. B., "Normal Mode Cycle Distance and Beam Displacement, Time Delay, etc. for Low (Non WKB) Frequencies," Journal of the Acoustical Society of America, V. 78 no. 3, September 1985.
5. Kinsler, L. E., Frey, A. R., Coppens, A. B., and Sanders, J. V., Fundamentals of Acoustics, 3rd Edition, John Wiley & Sons, 1982.
6. Urick, R. J., Principles of Underwater Sound, McGraw-Hill, 1975.
7. Eisberg, R. M., Applied Mathematical Physics with Programmable Pocket Calculators, McGraw-Hill, 1976.
8. Cooney, P. J., Kanter, E. P., and Vager, Z., "Convenient Technique for Solving the One Dimensional Schrödinger Equation for Bound States," American Journal of Physics V. 49 no. 1, January 1981.

# INITIAL DISTRIBUTION LIST

	No. Copies
1. Defense Technical Information Center Cameron Station Alexandria, Virginia 22304-6145	2
2. Superintendent Attn: Library, Code 0142 Naval Postgraduate School Monterey, California 93943-5002	2
3. Superintendent Attn: Chairman, Department of Physics (Code 61) Naval Postgraduate School Monterey, California 93943	2
4. Superintendent Attn: Professor A. B. Coppens (Code 61cz) Naval Postgraduate School Monterey, California 93943	5
5. Commander Attn: T. B. Gabrielson (Code 3031) Naval Air Development Center Warmister, Pennsylvania 18974	2
6. Commanding Officer Aurora Software Development Unit Canadian Forces Base Greenwood Greenwood, Nova Scotia Canada BOP 1N0	2
7. Canadian Forces Technical Library National Defence Headquarters Ottawa, Ontario Canada K1A 0K2	1
8. DPED National Defence Headquarters Ottawa, Ontario Canada K1A 0K2	1
9. Commandant Attn: H. J. Duffus Dean, Science and Engineering Royal Roads Military College FMO Victoria, British Columbia Canada VOS 1B0	1

- |     |   |   |
|-----|---|---|
| 10. | Commanding Officer<br>Acoustic Data Analysis Centre<br>Marcom HQ<br>Halifax, Nova Scotia<br>Canada B2K 2X0  | 1 |
| 11. | Commanding Officer<br>Attn: Oceanography Officer<br>HT406<br>CFB Shearwater<br>Nova Scotia<br>Canada B0J 3A0  | 1 |
| 12. | SPAWAR<br>Attn: Commander Charles Stehle<br>PBW 124 617<br>Washington, D.C. 20363-5100  | 1 |
| 13. | Attn: SSO Env.<br>Canadian Forces Maritime Warfare School<br>Canadian Forces Bases Halifax<br>Halifax, Nova Scotia<br>Canada B3K 2X0                | 1 |
| 14. | Capt. Sylvain Fleurant<br>25 Mynarski Cres.<br>Ottawa, Ontario<br>Canada KOA 2E2  | 1 |
| 15. | Mr. and Mrs. Douglas Cantley<br>General Delivery<br>Rocky Mountain House, Alberta<br>Canada T0J 1N0   | 1 |
| 16. | Captain Douglas Cantley<br>3 Fales River Drive<br>Greenwood, Nova Scotia<br>Canada B0P 1N0  | 6 |
| 17. | Captain Bruce Lewis<br>Defence Scientist<br>Defence Research Establishment Atlantic<br>4 Tummell Drive<br>Dartmouth, Nova Scotia<br>Canada B2X 2A8. | 1 |



40  
PL 17608/2











220957 67

Thesis  
C19455  
c.1

Cantley

A numerical method  
for solving for normal  
modes with impedance  
bottom.

3 MAY 39  
5 JULY 01

32966  
56145

220957

Thesis  
C19455  
c.1

Cantley

A numerical method  
for solving for normal  
modes with impedance  
bottom.



thesC19455

A numerical method for solving for norma



3 2768 000 75834 6

DUDLEY KNOX LIBRARY